Politecnico di Torino

Department of Environment, Land and Infrastructure Engineering



Master of science program in

GEORESOURCES AND GEOENERGY ENGINEERING

Surface wave analysis of marine seismic data - Scholte wave simulation

Supervisors:

Farbod Khosro Anjom

Evgenia Koutra

Laura Valentina Socco

Claudio Piatti



Acknowledgements

I would like to express my deepest gratitude to my supervisor, Farbod Khosro Anjom, for his invaluable expertise, continuous guidance, and patience throughout the course of this research. His insightful feedback and encouragement were instrumental in bringing this thesis to completion.

My sincere thanks also go to Claudio Piatti, Principal Engineer at GEOWYND, for his generous support in providing the data used in this study, as well as for his time, advice, and technical insights that greatly enriched this work.

I am profoundly grateful to my family and friends for their unwavering support, encouragement, and belief in me throughout the challenges and triumphs of this journey. Their constant presence made this accomplishment possible.

Finally, I wish to extend my heartfelt appreciation to Prof. Laura Valentina Socco, whose valuable counsel and thoughtful suggestions helped me overcome numerous obstacles during the research process. Her kindness and academic wisdom were a continual source of inspiration.

For the completion of the thesis are used computational resources provided by hpc@polito, which is a project of Academic Computing within the Department of Control and Computer Engineering at the Politecnico di Torino (http://www.hpc.polito.it).

Abstract

The study of geophysical properties of shallow marine environments is critical for characterising the subsurface in offshore sites for both the oil and gas industry and also the geotechnical characterisation of the soil for the construction of sites like the ones for off shore wind turbines. Due to the complexity of these environments, like heterogeneity of sediments and complex water-soil interactions, conventional seismic geophysical methods may be challenging, time consuming and costly. This thesis focuses on the importance of studying Scholte waves propagation along the seabed in order to successfully characterise shallow marine sediments.

This study is achieved through the creation of multi-layer 3D models with known density, P-wave velocity and S-wave velocity values from which the synthetic seismogram traces are produced using a Finite Difference Algorithm (FDA) provided by the SOFI3D software. The dispersion curves of the Scholte wave velocities are extracted and isolated at low frequencies to reveal a relationship between frequency and velocity. Through the process of inversion, the S-wave velocity versus depth profile is derived providing an insight into the subsurface volume and subsequently recognising any lateral variations and layering characteristics

Table of Contents

1. Ir	ntroduction	1
1.1	Motivation	1
1.2	Thesis Outline	3
2. St	urface Waves Overview – Scholte Waves	4
2.1	Surface Waves	4
2.2	Scholte Waves and Acquisition	4
3. M	1ethodology	6
3.1	Dispersion Curve	6
3.2	Forward Problem	7
3.3	Inverse Problem	8
3.	.3.1 Laterally Constraint Inversion (LCI)	8
3.4	SOFI3D Theoretical Background	9
3.	.4.1 The Courant's Instability	11
4. D	ata Sets	12
4.1	Data Set number 1	12
4.2	Data Set number 2	18
4.3	Data Set number 3	24
5. R	esults	29
5.1	Dataset number 1 DCs and Inversion	29
5.2	Dataset number 2 DC and Inversion	32
5.3	Dataset number 3 DC and Inversion	34
6. C	Conclusions	36
6.1	Final Remarks	36
6.2	Future Prospects	36
7 R	eferences	38

Tables

Table 1: Petrophysical properties of synthetic data number 1
Table 2: Acquisition parameters of dataset number 1
Table 3: Acquisition parameters of dataset number 2
Table 4: Petrophysical properties of synthetic data number 2
Table 5: Petrophysical properties of the five boulders inserted to the model24
Figures
Figure 2-1: Acquisition of Scholte Waves and acoustic guided waves in shallow marine
environments using the "stationary receiver method" and the "towed acquisition" with a fixed
source and streamer configuration records conventional shot-gathers. (Klein, et al., 2005) 5
Figure 2-2: The dispersion curve of Scholte and guided waves plotted together shows the
strong separation in velocity and in frequency for a shallow model. (Strobbia, et al., 2006) 5
Figure 3-1: Geometry of the numerical FD grid where on top of the numerical mesh the PEs
apply a free surface boundary condition similar to our study (Bohlen, et al., 2015)10
Figure 4-1: Distribution of S-wave velocity in m/s of the simple synthetic model 1 along y-z,
x-y and x-z plains of the 3D model of the subsurface
Figure 4-2: Distribution of P-wave velocity in m/s of the simple synthetic model 1 along y-z,
x-y and x-z plains of the 3D model of the subsurface
Figure 4-3: Distribution of density in kg/m3 of the simple synthetic model 1 along y-z, x-y
and x-z plains of the 3D model of the subsurface
Figure 4-4: Synthetic seismogram for simple synthetic model 1
Figure 4-5: Distribution of S-wave velocity in m/s of the synthetic model 2 along y-z, x-y and
x-z plains of the 3D model of the subsurface
Figure 4-6: Distribution of P-wave velocity in m/s of the synthetic model 2 along y-z, x-y and
x-z plains of the 3D model of the subsurface
Figure 4-7: Distribution of density in kg/m3 of the synthetic model 2 along y-z, x-y and x-z
plains of the 3D model of the subsurface
Figure 4-8: Synthetic seismogram for synthetic model 2
Figure 4-9: Distribution of S-wave velocity in m/s of the synthetic model 3 along y-z, x-y and
x-z plains of the 3D model of the subsurface. The boulders' vs is 1900 m/s, much higher than
x-2 plains of the 3D model of the subsurface. The bounders vs is 1900 m/s, much higher than

Figure 4-10: Distribution of P-wave velocity in m/s of the synthetic model 3 along y-z, x-y
and x-z plains of the 3D model of the subsurface. The boulders' vp is 3500 m/s, much higher
than the numbers on the axis, corresponding to the water, clay and sand values of 400-2000
m/s26
Figure 4-11: Distribution of density in kg/m3 of the synthetic model 3 along y-z, x-y and x-z
plains of the 3D model of the subsurface. The boulders' ρ is 2500 kg/m3, higher than the
numbers on the axis, corresponding to the water, clay and sand values of 1000-2000 kg/m3.
27
Figure 4-12: Synthetic seismogram for synthetic model 3
Figure 5-1: The DC of the horizontal component computed corresponding to synthetic model
1 as a function of frequency
Figure 5-2: The DC of the vertical component computed corresponding to synthetic model 1
as a function of frequency
Figure 5-3: The estimated Vs model for the simple synthetic model using LCI30
Figure 5-4: Comparison of experimental and computed Vs models for simple synthetic 131
Figure 5 5. The side 1 DCs
Figure 5-5: The picked DCs
Figure 5-5: The picked DCs
Figure 5-6: The DC of the vertical component computed corresponding to synthetic model 2
Figure 5-6: The DC of the vertical component computed corresponding to synthetic model 2 as a function of frequency. The spectra show multiple modes of excited Scholte waves which
Figure 5-6: The DC of the vertical component computed corresponding to synthetic model 2 as a function of frequency. The spectra show multiple modes of excited Scholte waves which match with the theoretical one (red line).
Figure 5-6: The DC of the vertical component computed corresponding to synthetic model 2 as a function of frequency. The spectra show multiple modes of excited Scholte waves which match with the theoretical one (red line)
Figure 5-6: The DC of the vertical component computed corresponding to synthetic model 2 as a function of frequency. The spectra show multiple modes of excited Scholte waves which match with the theoretical one (red line)
Figure 5-6: The DC of the vertical component computed corresponding to synthetic model 2 as a function of frequency. The spectra show multiple modes of excited Scholte waves which match with the theoretical one (red line)

1. Introduction

1.1 Motivation

The increasing global demand for renewable and sustainable energy in addition to the depletion of oil and gas reserves and the Net Zero EU policy are accelerating the development of new technologies that will solve the high energy demand of the population. Offshore wind farms are one of the fastest growing sectors (Barrett, Pye and Betts-Davies 2022) thanks to their remote location, low noise and visual pollution impacts and higher efficiencies for the production of electricity. According to the European Marine Observation and Data Network (EMODnet), offshore wind farms are successfully producing in the United Kingdom, the Netherlands and Germany while many more future projects are approved in Italy, Spain, Sweden and Finland.

However, the shallow marine environments in which the wind turbines are located, oppose difficulties in their construction and maintenance or long-term stability. Geophysical studies and especially near surface seismic methods can successfully characterise the subsurface volume, especially when petrophysical and geotechnical properties are already available.

The near surface geophysical seismic studies are critical and advantageous for subsurface characterisation. They offer high spatial resolution data, detecting lateral variations in sedimentary environments without needing a borehole intervention while being able to detect geological heterogeneities like buried channels or sediment layers (Steeples and R.D. 1998). They are non-intrusive (no drilling or coring) something extremely beneficial in marine areas, where it is essential to minimize any environmental impact and pollution. An important point, critical for this thesis is that they are directly sensitive to the elastic moduli of the soil. By analysing P-wave and S-wave velocities, parameters such as stiffness, density, and Poisson's ratio can be estimated. These properties are fundamental for geotechnical design of structures, including the analysis of soil stability, compaction, and load-bearing capacity (Bachrach and Nur 1998). The seismic inversion technique, which is part of the surface waves analysis, allows a quantitative estimation of subsurface parameters and enables the derivation of shear-wave velocity (Vs) profiles, which are essential for seismic site classification, dynamic soil

behaviour assessment, and foundation design (Park, Miller and Xia 1999) (S. Kugler, et al. 2007).

In this thesis the near surface seismic study used is the Scholte Waves Analysis. The study of subsurface can be achieved through the dispersion of Scholte waves, which are elastic interface waves that propagate along a fluid (water) and elastic solid medium (sand or sediments). Scholte-wave tomography has been successfully applied in shallow marine sediments to estimate 3D shear-wave velocity structures, where the waves were excited via air guns and recorded with ocean bottom seismometers and geophones, proving that it is well suited for geotechnical engineering applications in marine environments. (S. Kugler, et al. 2007). The Scholte waves are also relevant in understanding environmental noise, particle motion during offshore construction (pile driving), since they generate significant motion in the ocean bottom with maximum amplitude at seafloor and thus may contribute to potential impacts on marine life (Potty, et al. 2023).

In general, there are two main approaches for the S-wave velocity reconstruction using Scholte waves data, the dispersion curve (DC) analysis followed by inversion and the full waveform inversion (FWI). The FWI is a seismic imaging approach providing high resolution results which utilizes all kinds of waveforms (reflection and refraction waves) to reconstruct the subsurface velocity model (Fang, Fang and Demanet 2020). Despite the good lateral resolution, it is computationally heavy since the wave equation of the seismic wave needs to be solved many times and the cycle skipping risk is strong, since due to the non-linearity of the method, the inversion gets trapped in local minima (Brossier, Operto and Virieux 2009). To avoid these issues and to optimise the procedure of this thesis, the first approach is chosen. Last but not least, DC inversion is the appropriate method for a layered sedimentary subsurface volume, which can correspond to shallow marine environments.

Aim of this thesis is to generate synthetic models in a shallow marine environment, to study the propagation of Scholte waves on the seabed and how lateral variations can be recognised in order to give higher resolution data for integration with other geophysical and geotechnical data and improve offshore wind turbine sites characterisation.

1.2 Thesis Outline

A brief theoretical overview about surface and Scholte waves is given in chapter number 2.

The methodology followed is described in chapter 3, where more details are given on the geophysical process. The software used for the creation of the synthetic models is introduced as well as the theoretical background behind it, a general description of the dispersion curves and inversion process used to characterise the subsurface.

In chapter number 4, the synthetic models and simulated data are described. We created a total of three models and simulated the corresponding seismic datasets: a first simple laterally homogeneous elastic model with vertical variation of density and velocities for each layer by depth, a second more complex one based on real data from an anonymous site in South China Sea provided by Geowynd with varying values of density, P-wave and S-wave velocities and a third one where lateral variation is introduced in this dataset in the form of boulders.

In the next chapter, the results of the geophysical process for the three datasets along with the dispersion curves and the inversion product for each one of them and some remarks are provided.

Chapter number 6 presents the conclusion and discussion about future research and applications on the topic investigated.

2. Surface Waves Overview – Scholte Waves

2.1 Surface Waves

The investigation of the subsurface through surface waves (SW) depends on the principle that they propagate horizontally along a free surface and their energy decays with depth. These waves differ from body waves like P- and S- waves that travel through the bulk of the medium, propagating in all directions from the source. There are many types of SWs like Rayleigh, Love, Stoneley and Scholte, that differ in the medium in which they propagate or their particles motion. They are properly suitable for geometrical characterisation since they have a lower rate of geometrical attenuation due to their pattern of propagation.

2.2 Scholte Waves and Acquisition

Normally, two types of dispersive seismic waves are excited during the investigation of the seabed, the Scholte and P-guided waves. Scholte waves are observed at low frequencies and low phase velocities (close to sediments velocities), while their dispersion is mainly controlled by the depth profile of the shear-wave velocity (Figure 2-2). Acoustic guided waves show large amplitude variations over a broad frequency range and are more sensitive to P-wave velocity. Due to this large gap, especially in the DC investigation, the P-guided waves are discarded in this study. A typical configuration of data acquisition, proposed by (Klein, et al. 2005) is a stationary array of hydrophones and a moving source in order to produced common receiver gather and another array of streamers with fixed source to record conventional shot-gathers (Figure 2-1). Due to the simulation software's limitations and to optimise the study, the configuration is placed on the seabed and no floating arrays have been considered.

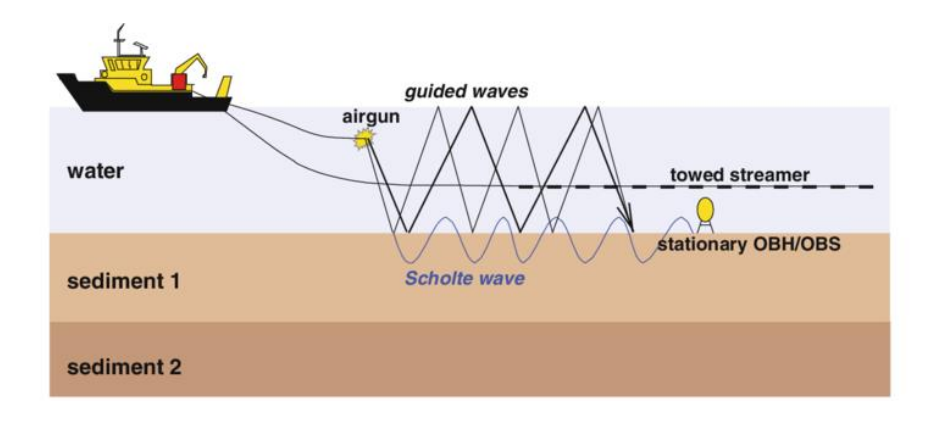


Figure 2-1: Acquisition of Scholte Waves and acoustic guided waves in shallow marine environments using the "stationary receiver method" and the "towed acquisition" with a fixed source and streamer configuration records conventional shot-gathers. (Klein, et al. 2005)

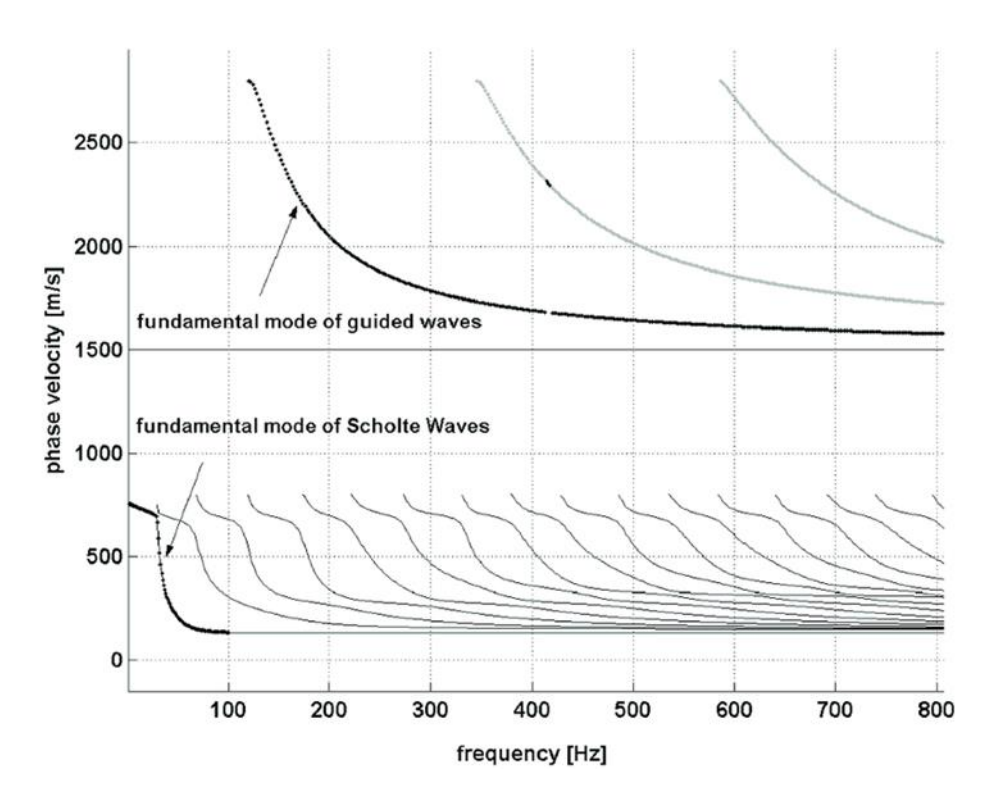


Figure 2-2: The dispersion curve of Scholte and guided waves plotted together shows the strong separation in velocity and in frequency for a shallow model. (Strobbia, Godio and De Bacco 2006)

3. Methodology

The geophysical process for the surface wave analysis which also applies for Scholte waves (our approach for shallow marine environment) is standard and follows three main steps. The first step is the data acquisition which in this case are synthetic and not experimental. The second step is the extraction of the dispersion curve after processing the data, which is a curve expressing the relationship between the frequencies and their respective phase velocities, caused by the geometric dispersion of the wave. Third and last step is the inversion process through which the model parameters of interest are estimated. In surface wave analysis by inverting the dispersion curves the shear wave velocities can be estimated for the characterisation of the subsurface (Aki and Richards 1980).

Surface wave methods (SWMs) generally utilize the dispersive nature of surface waves in a layered medium to obtain a shear wave velocity (Vs) profile (Wisen and Christiansen 2005), through an inversion step. There are various inversion algorithms both stochastic and deterministic. Lateral Constrained Inversion (LCI) is a common deterministic approach to obtain a laterally consistent model. Surface wave methods have been under development for several decades, and a thorough and up to date description of the available techniques is found in (Socco and Strobbia, Surface-wave method for near-surface characterization: a tutorial 2004).

3.1 Dispersion Curve

Dispersion refers to the phenomenon by which the phase velocity (v_p) depends on its frequency. Phase velocity is the rate at which the wave propagates in any medium,

$$\nu_p = \frac{\lambda}{T} \tag{3.1}$$

where λ is the wavelength and T the time period.

In a dispersive medium, different frequencies travel at different speeds and the dispersion curves (phase velocity vs frequency) are characteristic of the medium. In Scholte waves, which are interface waves, the frequency-dependent behaviour is produced from the contrast between the fluid and solid medium.

In this thesis the dispersion curve is calculated based on the phase shift method, also known as the wavefield transformation method by (Park, Miller and Xia 1999). It is a wave transformation technique to obtain a phase-velocity spectra (dispersion image) based on a multichannel impulsive shot gather. The frequency-phase velocity spectrum is obtained by integrating the Fourier transform of the traces over the offset:

$$s(\omega, c) = \int e^{(-i(\omega/c)x)} * u(x, \omega) dx$$
 (3.2)

where u is the phase component of the Fourier transform, ω is the angular frequency and c the phase velocity. The dispersion curve is picked as the local maxima at each frequency.

For our recordings we have spatial windowing (DC picking for every 25 receivers), where the Fourier transform is applied and the DCs are estimated for that window something that allows us to obtain many DCs, depicting the lateral variation. In order to optimise the process, an algorithm is used which allows an automatic picking of the generated DCs within the defined windows.

3.2 Forward Problem

The surface wave dispersion curve analysis involves a forward and inverse problem. The forward refers to the creation of a synthetic DC from a known model and it was computed by an algorithm introduced by (Thomson 1950) and modified by (Haskell 1953). This method constructs a series of transfer matrices that encapsulate the propagation of stress and displacement fields across each layer. By enforcing the continuity of these fields at layer interfaces, the system of equations is condensed into a single, global system matrix that relates the wavefields at the top and bottom of the entire model stack. The existence of surface wave modes corresponds to the non-trivial solutions of this system, which occurs when the determinant of the system matrix is zero. This Haskell-Thomson determinant is a function of angular frequency (ω) and wavenumber (k), and its roots define the modal dispersion solutions.

In our case, the forward problem involves generating the synthetic dataset and extracting the direct component from the synthetic seismogram to support the interpretation of the Vs.

3.3 Inverse Problem

By inversion in the DC analysis, we aim to find a realistic model with a synthetic DC that better fits our experimental one. In general, the term inversion means the 'estimation of the parameters of a postulated earth model from a set of observations' (Lines and Treitel, 1984). It is fundamentally a mathematical optimization problem which gives a synthetic model of the subsurface as similar as possible to the experimental one. The inverted model can be interpreted directly for the physical features that it describes.

The inverse algorithms are classified as stochastic or deterministic. The deterministic methods employ a Newtonian approach. The process begins with the initial guess of the subsurface model. The forward algorithm, as described previously, is used to compute a synthetic DC for this starting model. This synthetic DC is then compared against the experimentally observed DC, and the difference is quantified by a misfit function. In contrast to deterministic approaches, stochastic inversion methods for surface wave analysis are fundamentally rooted in sampling-based techniques, with the Monte Carlo method being the most used (Sambridge and Mosegaard 2002). These algorithms explore the model space by generating a vast ensemble of candidate models, whose parameters are randomly drawn from predefined probability distributions. Each model is evaluated by computing its synthetic dispersion curve and calculating a data misfit, often transformed into a likelihood or posterior probability. The solution is not a single "best-fit" model but rather a collection of models that satisfactorily explain the observed data. In our study the Laterally Constraint Inversion (LCI) is used where we extract the characteristics of the shallow environment through a deterministic inversion of the DC.

3.3.1 Laterally Constraint Inversion (LCI)

The term laterally constrained inversion (LCI) refers to inverting data along a profile by minimizing a common objective function (Auken and Christiansen 2004). According to (Wisen and Christiansen 2005) the LCI is a «parameterized inversion of data of the same type with lateral constraints on the model parameters between neighbouring models». Moreover, the lateral constraints can be considered as a priori information on the geological variability within

the investigated area; the smaller the expected variation of a model parameter, the more rigid the constraint, while the resulting model section is laterally smooth with sharp layer interfaces.

In our study a deterministic least squared LCI algorithm is followed, which is developed by (Socco, Boiero, et al. 2009), based on the work of (Auken and Christiansen 2004).

LCI solves an overdetermined problem (i.e., there are more data than model parameters), a sensitivity analysis of the estimated model parameters is performed, which is a linearized approximation of the covariance of the estimation error C_{est} (Tarantola and Valette, 1982):

$$C_{est} = (G'^T C' G')^{-1}$$
 (3.3)

where G'G'G' contains the Jacobian, the a priori information, and the regularization terms, while C'C'C' contains the experimental uncertainties, the uncertainties on the a priori information, and the constraints (Auken and Christiansen 2004). The standard deviations of the model parameters are calculated as the square roots of the diagonal elements of C_{est}.

3.4 SOFI3D Theoretical Background

In order to simulate the propagation of elastic waves and produce synthetic experimental data, the numerical modelling software SOFI3D was used which is based on the elastic and viscoelastic finite difference approach proposed by (Virieux 1986) and (Levander 1988). In Finite Difference algorithms derivatives are approximated using values of a function at discrete points. Instead of solving a continuous derivative it is approximated by a limit with a small finite step, so that differential equations are solved numerically by a computer. In our case, the elastic wave equations (3.4) and (3.5) are solved by calculating the particles velocities ν , the stresses Pij, and the Lamé parameters μ and λ at discrete cartesian coordinates and discrete times on a grid. By running the program, the partial derivatives are replaced by finite difference operators. The geometry of the numerical grid is presented on Figure 3-1.

The equation that describes the microscopic motion of the particles which predicts the particle displacements and therefore the propagation of the seismic wave in the rock is:

$$\rho \frac{dv_i}{dt} + v_i \rho \nabla v_i = -\frac{\partial p_{ij}}{\partial x_i} + f_i$$
 (3.4)

where the stress-strain relationship (surface forces) is described by p_{ij} , and f_i the forces acting on all the particles in the volume (body forces). This equation is satisfied no matter the phase of saturation of the subsurface volume (gas, liquid or rock).

Furthermore, for an elastic medium the stress-strain relationship is described by a linear equation:

$$P_{ij} = \lambda \theta \delta_{ij} + 2\mu \varepsilon_{ij} \tag{3.5}$$

Where λ and μ are the Lamé parameters, ε_{ij} the deformation tensor, θ the cubic dilatation and δ_{ij} the Kronecker symbol.

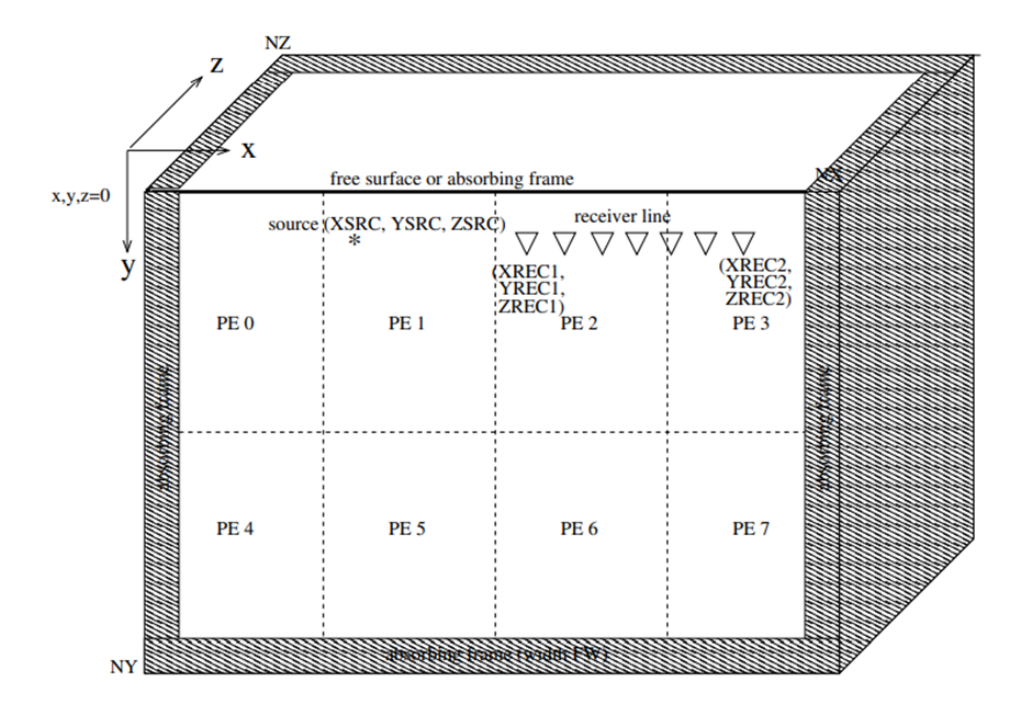


Figure 3-1: Geometry of the numerical FD grid where on top of the numerical mesh the PEs apply a free surface boundary condition similar to our study (Bohlen, et al. 2015)

3.4.1 The Courant's Instability

The software in order to ensure the stability of the simulation and the FD code, takes into consideration that the parameters chosen to satisfy a sampling criterion. This criterion is called Courant Friedrichs-Lewy criterion and according to it, if a wave is crossing a discrete grid, then the timestep dt must be less than the time for the wave to travel between two adjacent grid points with grid spacing dh. For a 3-D grid this means mathematically:

$$dt \le \frac{dh}{r_{max} * v_{p,max}} \tag{3.6}$$

Where $v_{p,max}$ is the maximum P-wave velocity in the model and the factor r_{max} represents the Courant-Friedrichs-Lewy (CFL) number. The factor r is chosen depending on the FD operator lengths and types (Taylor and Holberg operators).

In case that the Courant criterion is violated the amplitudes of the pressure field grow to infinity and the simulation immediately crashes due to unstable calculations.

This was critical when choosing the sampling rate for our models in this study.

4. Data Sets

The Scholte waves analysis is applied in three synthetic datasets simulations. The first corresponds to a simplified four layered model, laterally homogeneous where the petrophysical properties vary by depth for each layer, the second is a real case dataset simulating an anonymized real site in South China Sea, provided by Geowynd, with alternating clay and sand layers, laterally homogeneous, where the petrophysical properties vary gradually with depth and in the third model, lateral variations are introduced in the form of five shallow boulders, buried in the seabed. All three simulations are based on elastic wave propagation principles.

4.1 Data Set number 1

A 3D model is created using the MATLAB software, where the properties of the system are defined following Table 1. The dataset describes an ideal and simplified shallow marine environment of 102.4 x 51.2 x 51.2 m (length x depth x width in meters) with 4 layers and more specifically the chosen petrophysical properties are chosen as shown on Table 1.

Layers	Thickness (m)	Vs (m/s)	Vp (m/s)	Density (kg/m3)
Water	15	0.0001	1500	1000
Sand_1	10	100	1600	1800
Sand_2	10	300	1800	1900
Bedrock	16.2	1400	2500	2200

Table 1: Petrophysical properties of synthetic data number 1

They correspond to expected values of properties for water, sand and bedrock. There are no heterogeneities that always accompany sediments.

The values of the matrix are the inputs for the SOFI3D software in order to start the numerical simulation and extract the synthetic seismograms for further analysis.

The acquisition parameters for the seismic line are shown on Table 2.

	Recievers	Reciever Spacing (m)	Sources	Source Shape	Source Frequency (Hz)	Number of recievers		1 0
ı	Ocean Bottom Nodes (OBN)	1	Force on seabed	Ricker	20	91	1	0.18

Table 2: Acquisition parameters of dataset number 1

The seismic array of receivers and 20 Hz source is fixed on the seabed, located in the middle of the z direction, the width. Same logic applied to the rest of the models.

The source function is a Ricker wavelet and the equation is given as:

$$r(\tau) = (1 - 2\tau^2) \exp(-\tau^2) \tag{4.1}$$

with
$$\tau = \frac{\pi(t - \frac{1.5}{f_c} - t_d)}{1.0/f_c}$$
 (4.2)

where t denotes time, $f_c = 1/TS$ is the centre frequency, TS the duration time and t_d is a time delay which can be defined for each source position.

For a better visualisation the plots corresponding to the S-wave, P-wave velocities and densities are given for the x-y, y-z and x-z plain of the 3D model on Figures 4-1,4-2 and 4-3.

For all models is assumed as boundary condition one free surface which is the water surface.

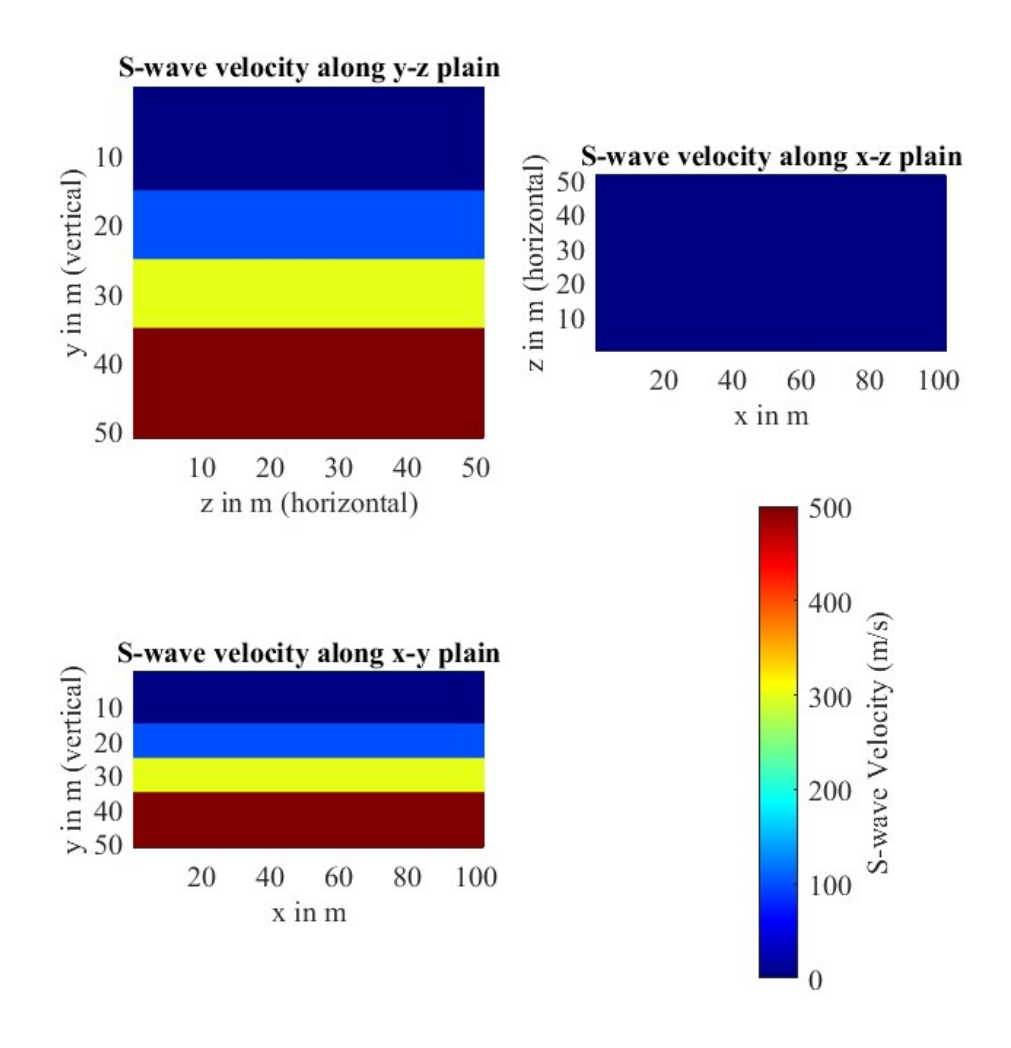


Figure 4-1: Distribution of S-wave velocity in m/s of the simple synthetic model 1 along y-z, x-y and x-z plains of the 3D model of the subsurface

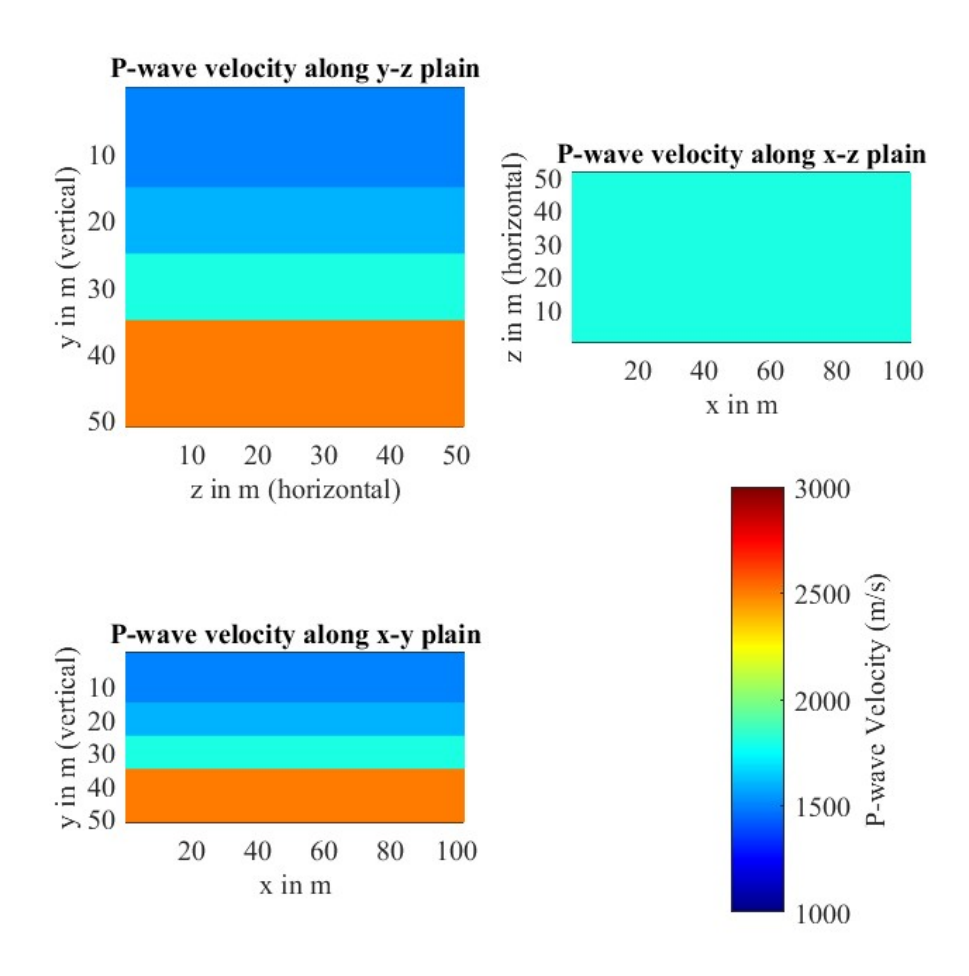


Figure 4-2: Distribution of P-wave velocity in m/s of the simple synthetic model 1 along y-z, x-y and x-z plains of the 3D model of the subsurface

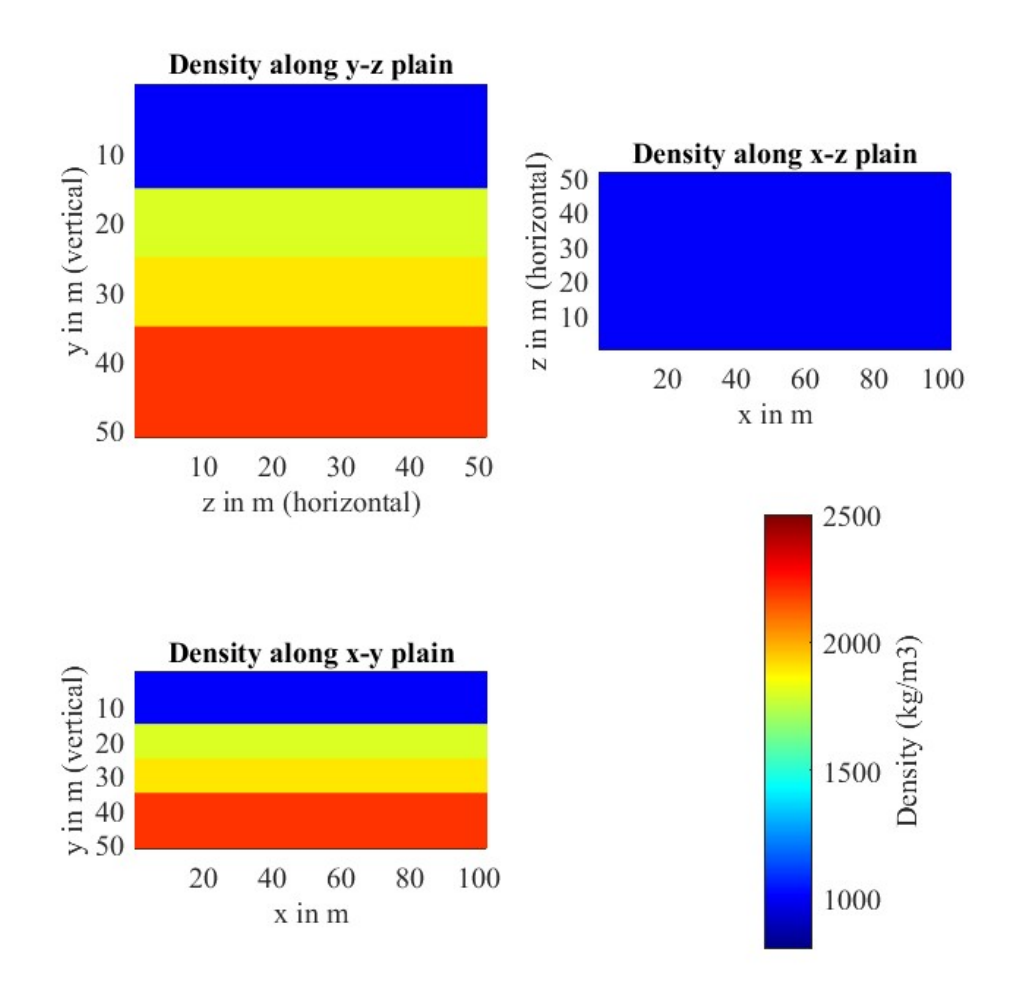
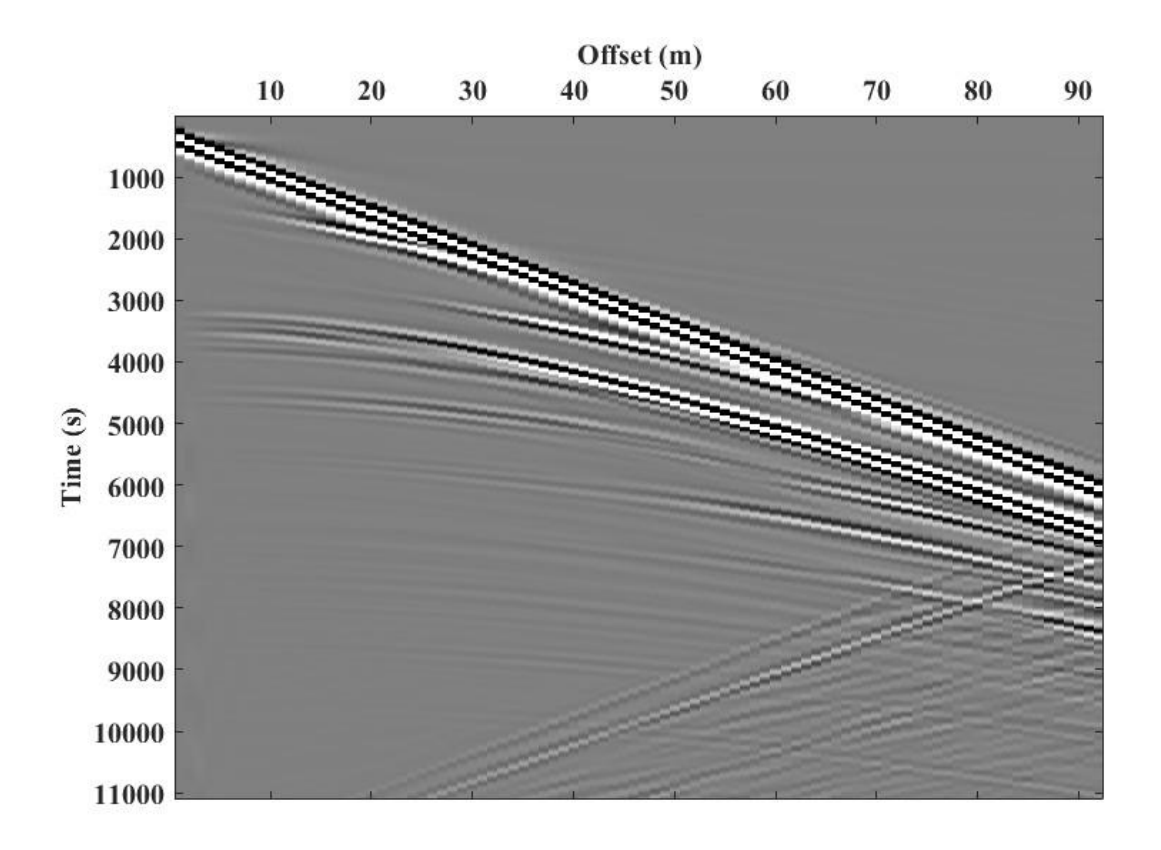


Figure 4-3: Distribution of density in kg/m^3 of the simple synthetic model 1 along y-z, x-y and x-z plains of the 3D model of the subsurface

The seismogram along the horizontal component (x) shown on Figure 4-4 is the product of the wave propagation simulation from SOFI3D. The main event, which is the Scholte wave, is represented as a straight line, while the hyperbolas are the multiple reflections from the water level.



Figure~4-4: Synthetic~seismogram~for~simple~synthetic~model~l

4.2 Data Set number 2

A second 3D model is created using the MATLAB software, where the properties of the system are defined following Table 4 provided by Geowynd. The dataset describes a shallow marine anonymized site in the Far East and more specifically at South China Sea, of 204.8 x 70 x 51.2 m (length x depth x width in meters), where Vs and density change with depth. In this study Vp is calculated from Poisson's ratio given the equation:

$$V_p / V_s = \sqrt{(1 - v) / (1/2 - v)}$$
 (4.3)

where Vp is the P-wave velocity, Vs is the S-wave velocity and v is Poisson's ratio.

This equation is derived from the fundamental elastic constants in isotropic materials, relating the bulk modulus (K), shear modulus (G), and density (ρ).

The acquisition parameters for the seismic line are shown on Table 3

Recievers	Reciever Spacing (m)	Sources	Source Shape	Source Frequency (Hz)	Number of recievers		1 0
OBN	1	Force on seabed	Ricker	20	184	1	0.18

Table 3: Acquisition parameters of dataset number 2

At Image 1, it is shown the location from which the data come from.



Image 1: Satellite image indicating the approximate location from which the experimental data used for the second model are taken from (Google Maps)

Layer	Layer thickness (m)	rho (kg/m3)	vs (m/s)	vp (m/s)	Poisson ratio v
Water	20	1000	0.0001	1500	-
Sand	0.50	1916	90	459	0.48
Sand	0.50	1916	100	510	0.48
Sand	0.50	1916	100	510	0.48
Sand	0.70	1916	115	586	0.48
Sand	0.60	1916	115	586	0.48
Sand	0.54	1916	115	586	0.48
Sand	1.02	1927	120	612	0.48
Sand	0.96	1926	150	765	0.48
Sand	1.48	1926	170	867	0.48
Sand	1.40	1926	170	867	0.48
Sand	1.50	1926	180	918	0.48
Sand	1.46	1926	180	918	0.48
Sand	0.98	1845	195	994	0.48
Sand	1.26	1926	195	994	0.48
Sand	1.26	1926	195	994	0.48
Clay	1.36	1978	195	994	0.48
Sand	1.24	1855	200	1020	0.48
Clay	1.04	1966	205	1045	0.48
Clay	1.02	1966	205	1045	0.48
Sand	0.50	1845	220	1122	0.48
Clay	0.88	2039	220	1122	0.48
Clay	0.86	2039	220	1122	0.48
Clay	1.74	2039	220	1122	0.48
Clay	1.74	2039	220	1122	0.48
Clay	1.06	1978	260	1326	0.48
Sand	1.24	1926	260	1326	0.48
Sand	0.98	1855	260	1326	0.48
Sand	2.52	1926	290	1479	0.48
Sand	0.78	1855	290	1479	0.48
Sand	1.94	1926	290	1479	0.48
Clay	1.98	1957	300	1530	0.48
Sand	2.86	1845	320	1632	0.48
Sand	1.62	1926	330	1683	0.48
Sand	0.90	1937	330	1683	0.48
Sand	2.28	1886	330	1683	0.48
Sand	2.50	1886	330	1683	0.48
Sand	2.60	1886	330	1683	0.48
Clay	0.90	1988	340	1734	0.48
Clay	1.50	1937	340	1734	0.48
Sand	1.44	1886	340	1734	0.48

Table 4: Petrophysical properties of synthetic data number 2

For a better visualisation the plots corresponding to the S-wave, P-wave velocities and densities are given on Figures 4-5, 4-6 and 4-7.

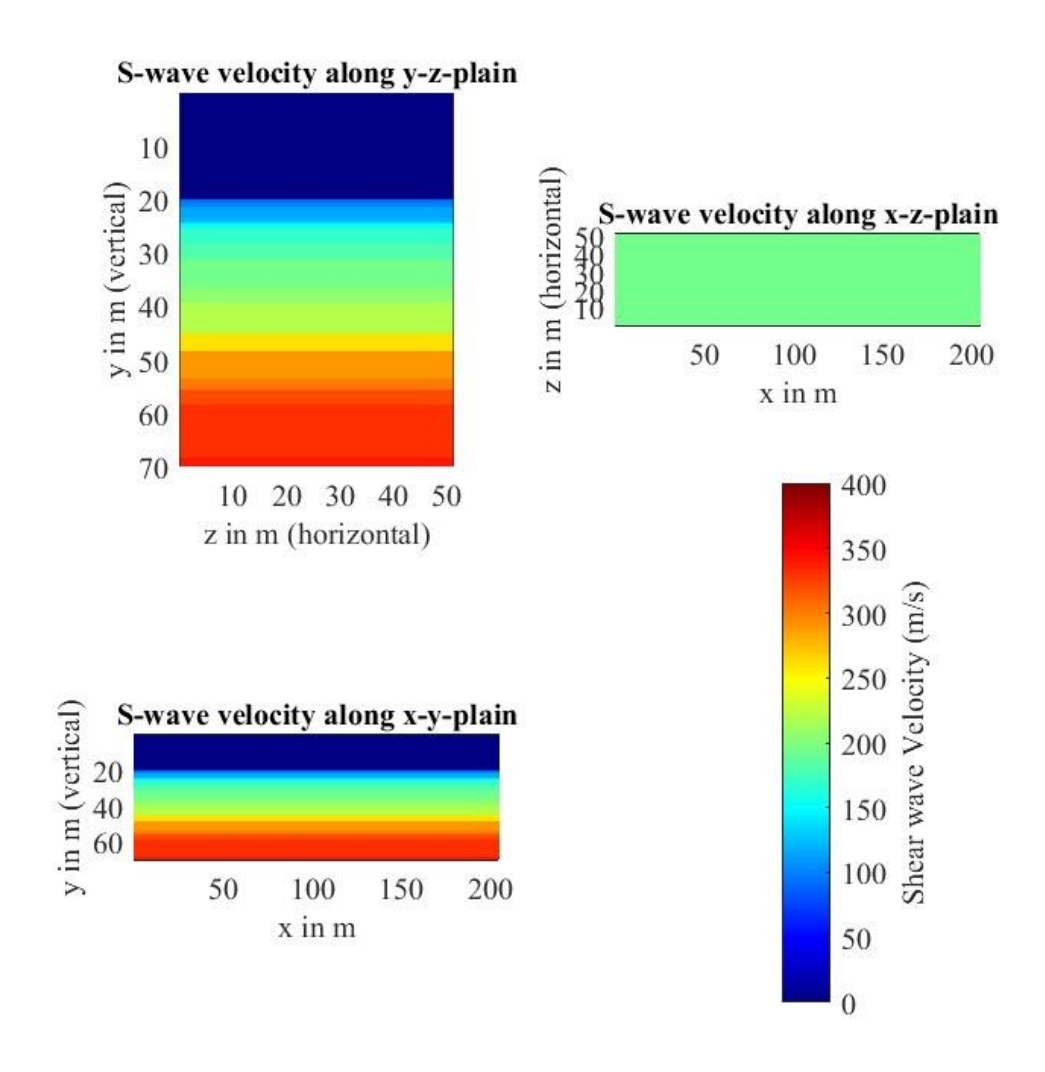


Figure 4-5: Distribution of S-wave velocity in m/s of the synthetic model 2 along y-z, x-y and x-z plains of the 3D model of the subsurface

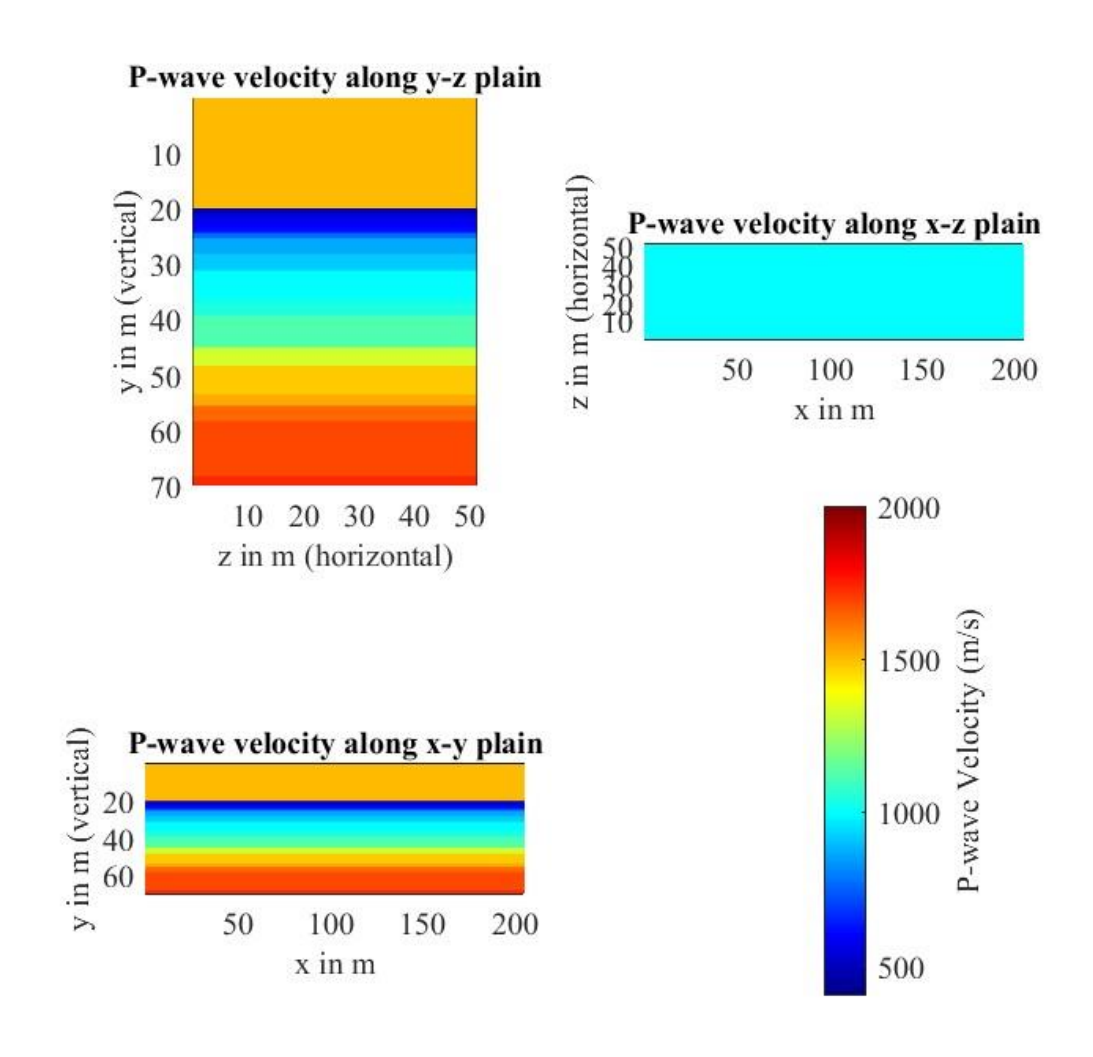


Figure 4-6: Distribution of P-wave velocity in m/s of the synthetic model 2 along y-z, x-y and x-z plains of the 3D model of the subsurface

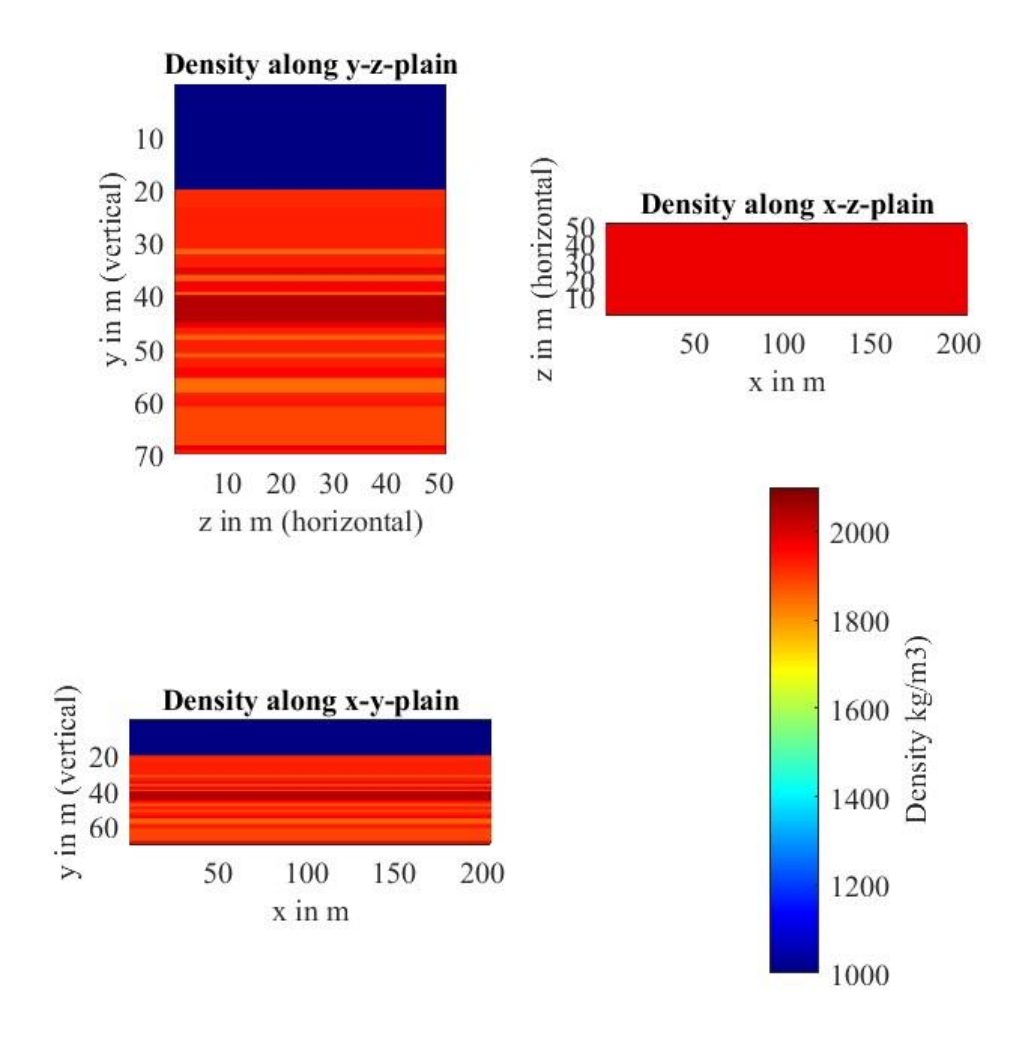


Figure 4-7: Distribution of density in kg/m^3 of the synthetic model 2 along y-z, x-y and x-z plains of the 3D model of the subsurface

The seismogram along the horizontal component (x) shown on Figure 4-8. The main event, which is the Scholte wave, is represented as a straight line, while the hyperbolas are the multiple reflections from the water level.

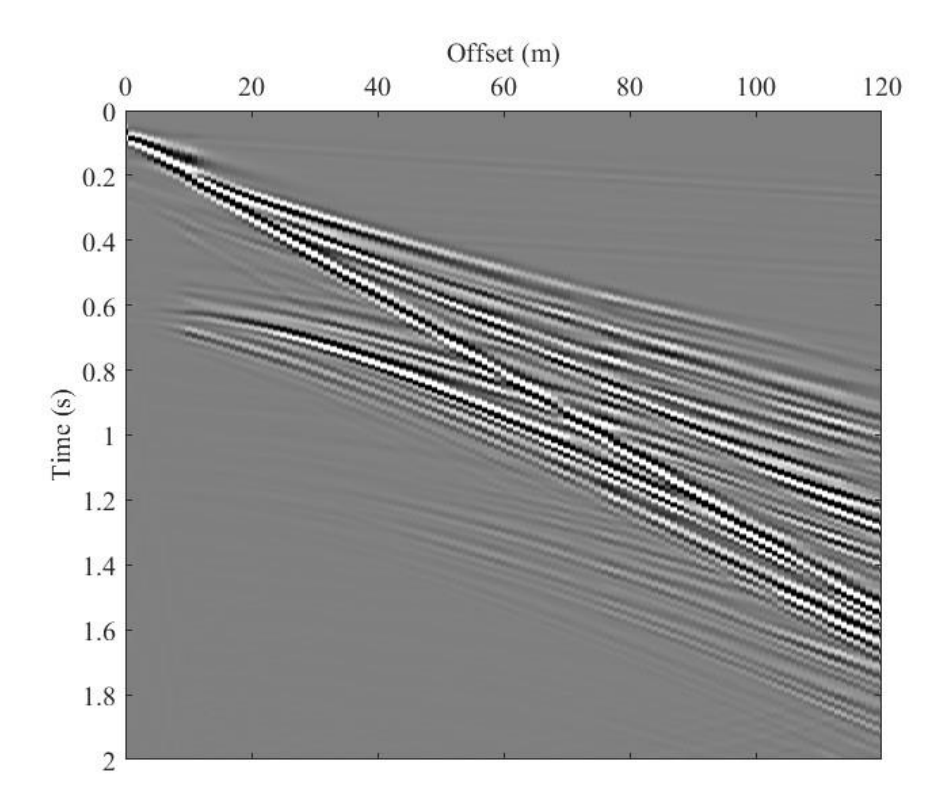


Figure 4-8: Synthetic seismogram for synthetic model 2

4.3 Data Set number 3

For the final dataset, five boulders in shallow depth are added to the model number 2 in order to spot any lateral variations and conclude the purpose of this study. The receivers and source array configuration remains the same as in Table 3 except of the sampling rate which is reduced to 0.095 ms and the five boulders, which are the geological heterogeneity in our case, are spherical and their centre is placed right underneath the configuration for the sake of simplicity. All of them have the same petrophysical properties and are placed in varying depths along the x-y plain. The characteristics are shown in detail on Table 5.

Boulder	Depth under the seabed (m)	Horizontal distance (m)	Radius (m)	Vs (m/s)	Vp (m/s)	Density (kg/m3)
1	6	50	4	1900	3500	2500
2	8	80	5	1900	3500	2500
3	4	102.4	3	1900	3500	2500
4	7	130	5	1900	3500	2500
5	5	160	4	1900	3500	2500

Table 5: Petrophysical properties of the five boulders inserted to the model

For a better visualisation the plots corresponding to the S-wave, P-wave velocities and densities are given on Figures 4-9, 4-10 and 4-11.

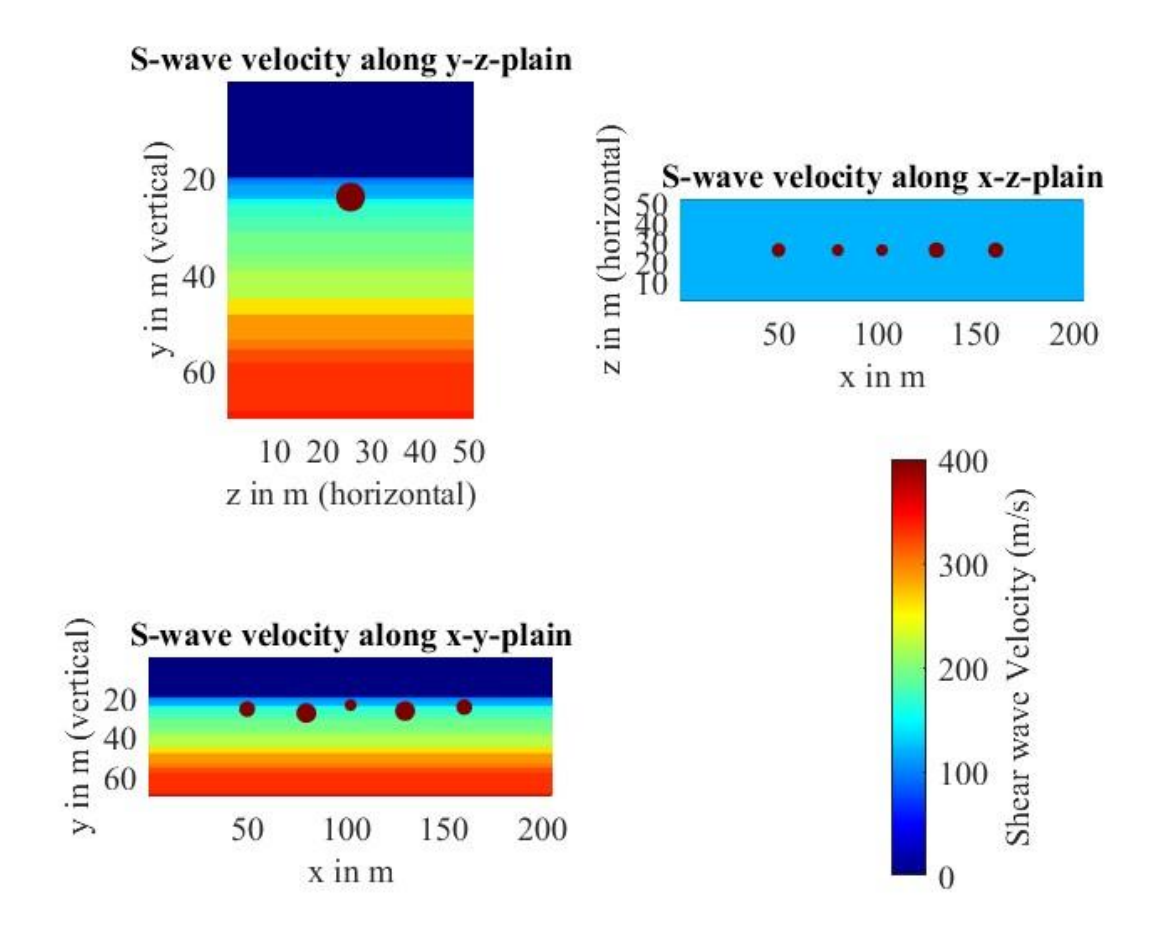


Figure 4-9: Distribution of S-wave velocity in m/s of the synthetic model 3 along y-z, x-y and x-z plains of the 3D model of the subsurface. The boulders' vs is 1900 m/s, much higher than the numbers on the axis, corresponding to the water, clay and sand values of 0-400 m/s.

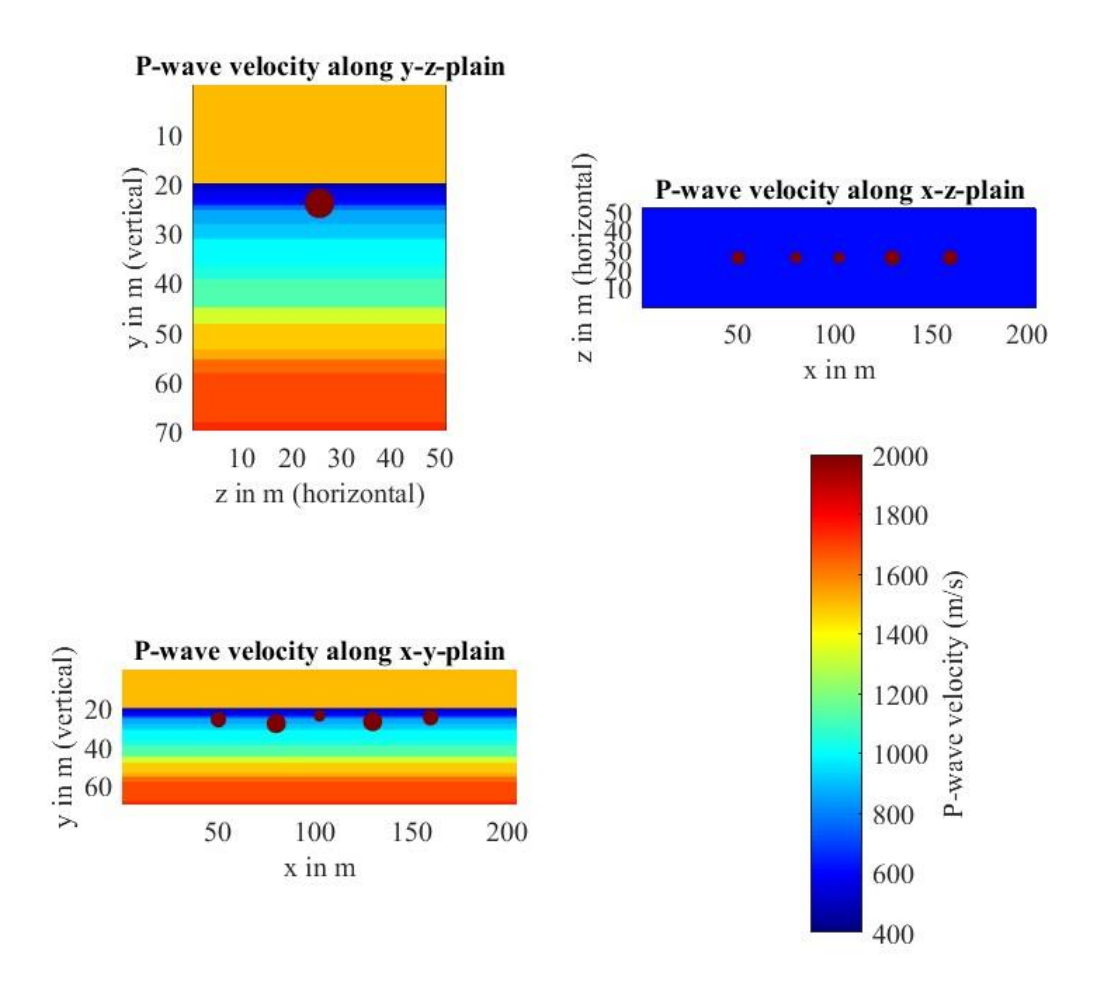


Figure 4-10: Distribution of P-wave velocity in m/s of the synthetic model 3 along y-z, x-y and x-z plains of the 3D model of the subsurface. The boulders' vp is 3500 m/s, much higher than the numbers on the axis, corresponding to the water, clay and sand values of 400-2000 m/s.

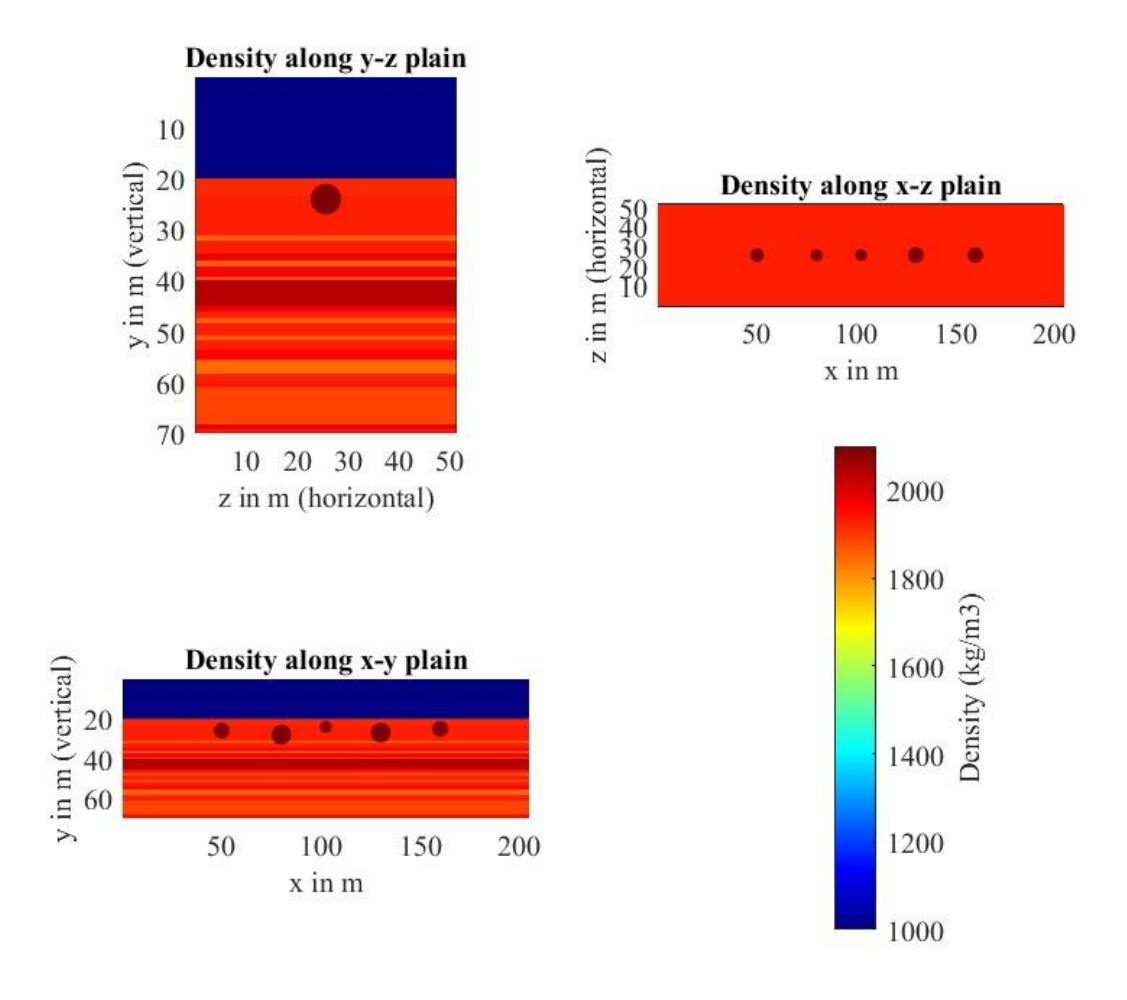


Figure 4-11: Distribution of density in kg/m^3 of the synthetic model 3 along y-z, x-y and x-z plains of the 3D model of the subsurface. The boulders' ρ is 2500 kg/m3, higher than the numbers on the axis, corresponding to the water, clay and sand values of 1000-2000 kg/m3.

The seismogram along the horizontal component (x) is shown on Figure 4-12. The Scholte wave is represented as a straight line, while the sharp hyperbolas at offset 40, 90 and 120 are related to the back reflections from the boulders. The other hyperbolas are related to the multiple reflections from the water level.

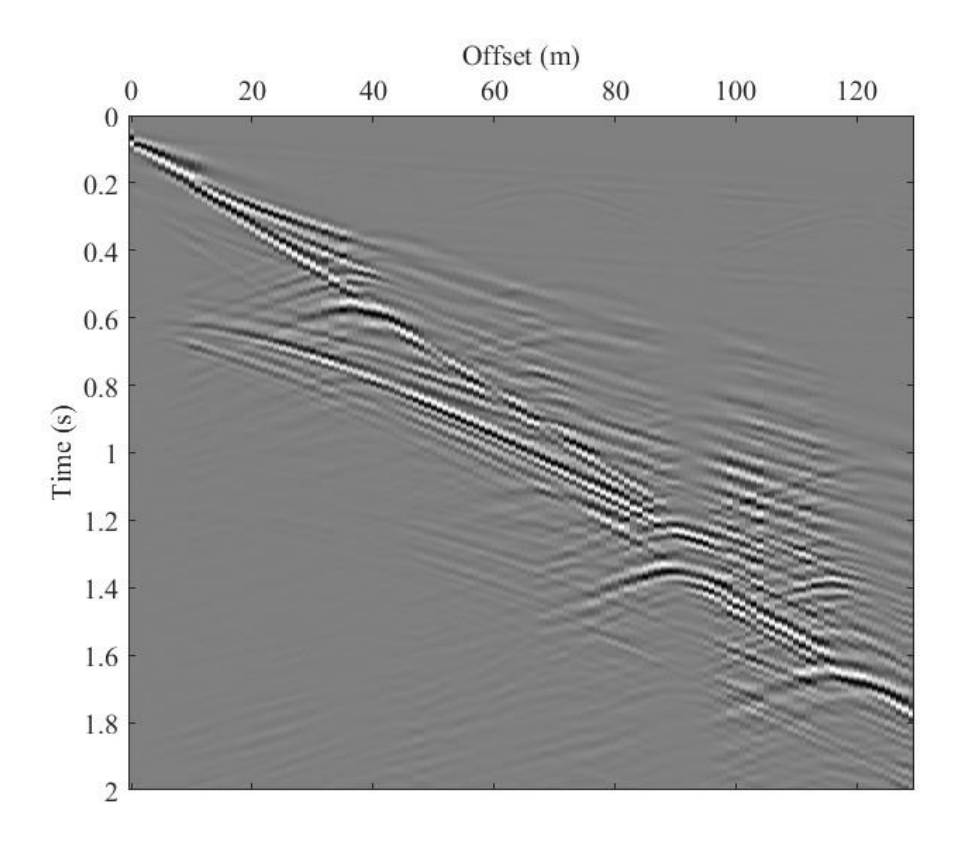


Figure 4-12: Synthetic seismogram for synthetic model 3

5. Results

In this chapter the DC extracted are presented along with the LCI results.

5.1 Dataset number 1 DCs and Inversion

The phase-velocity spectra generated by the phase-shift method in the velocity-frequency (v-f) domain for both the horizontal and vertical component, are shown on Figures 5-1 and 5-2 respectively. The red dotted line corresponds to the theoretical fundamental-mode DC.

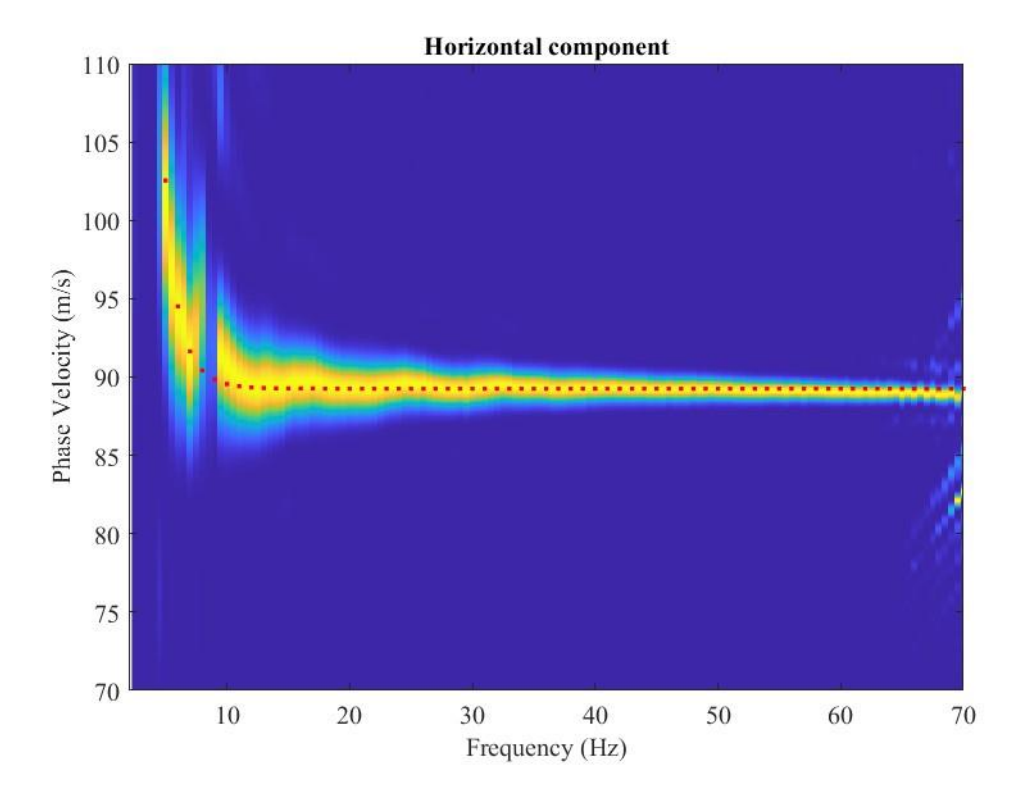


Figure 5-1: The DC of the horizontal component computed corresponding to synthetic model 1 as a function of frequency

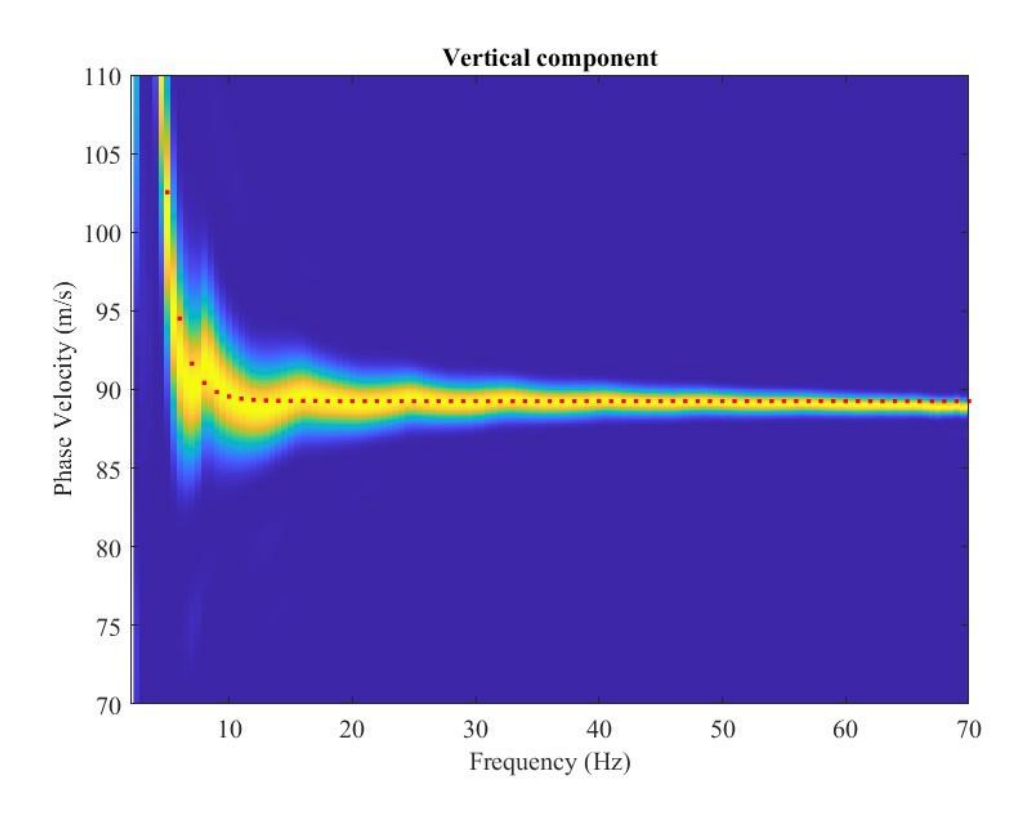


Figure 5-2: The DC of the vertical component computed corresponding to synthetic model 1 as a function of frequency

In figure 5-3, the result of the LCI is shown. It is observed that the inverted model approaches the experimental Vs model. The comparison between the two is shown in Figure 5-4.

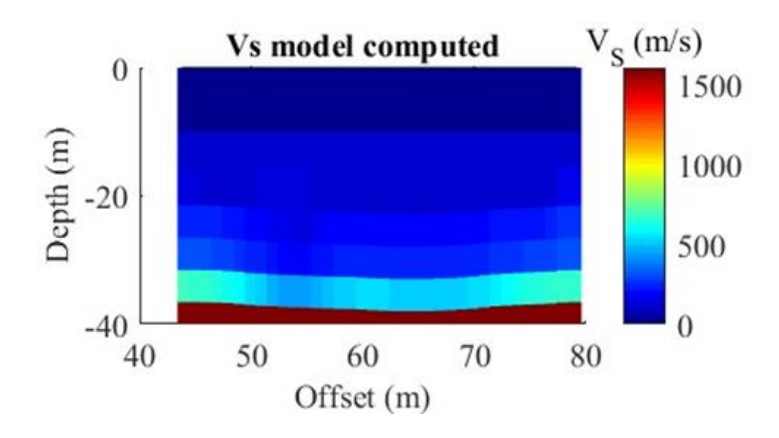


Figure 5-3: The estimated Vs model for the simple synthetic model using LCI

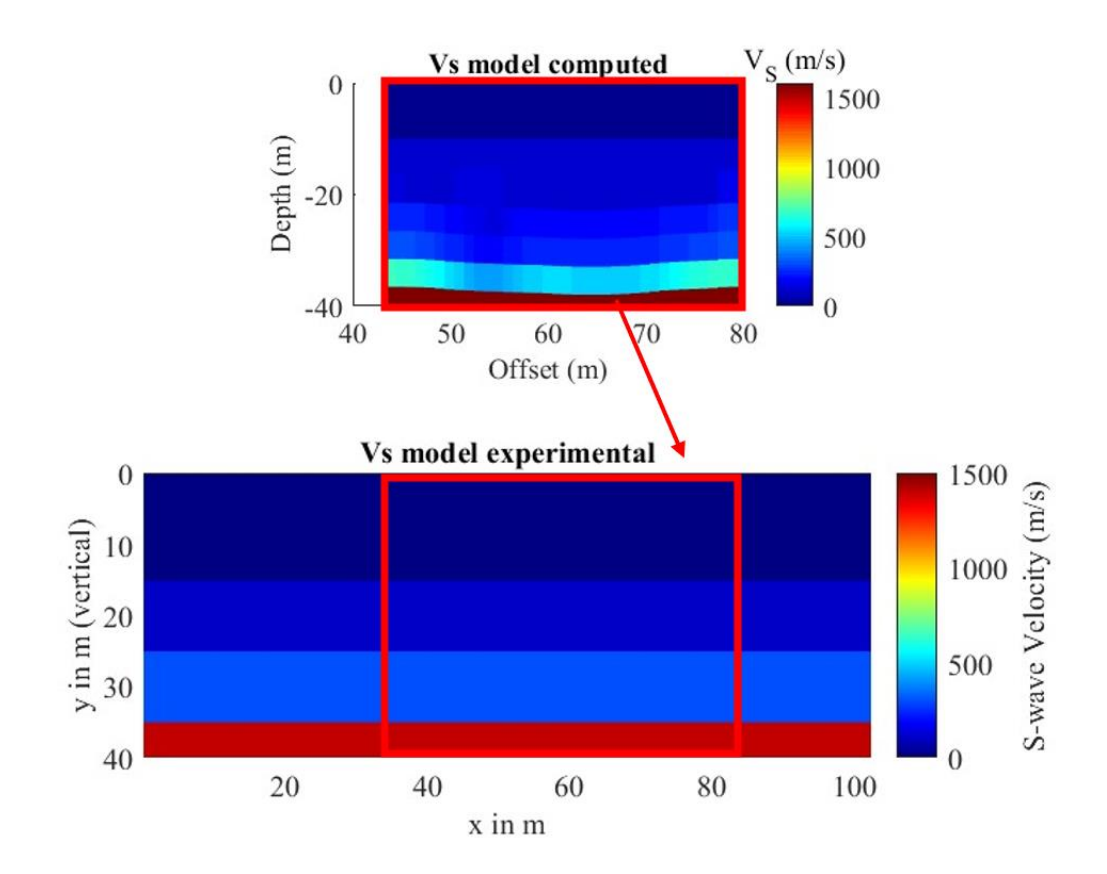


Figure 5-4: Comparison of experimental and computed Vs models for simple synthetic 1

5.2 Dataset number 2 DC and Inversion

The estimated phase-velocity spectra generated by the phase-shift method in the velocity-frequency (v-f) domain for the horizontal component is shown in Figures 5-5 and 5-6.

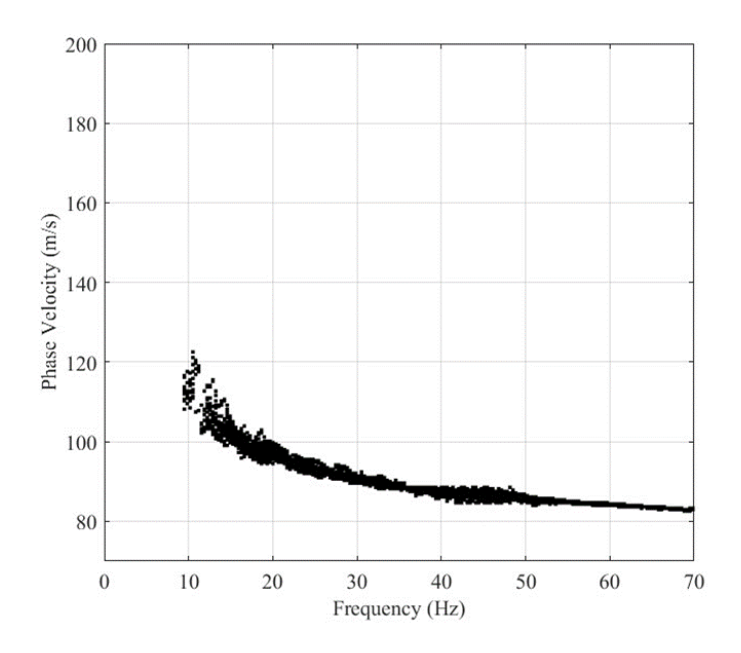


Figure 5-5: The picked DCs

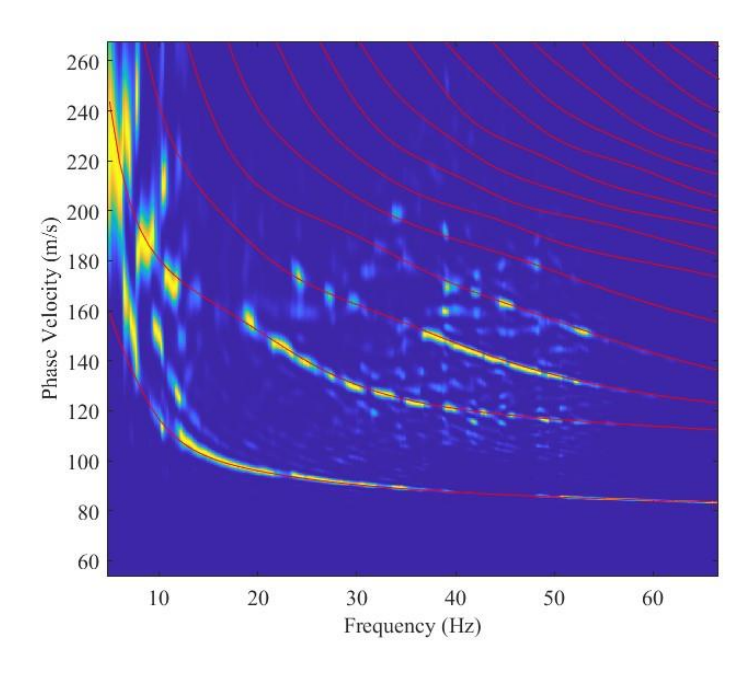


Figure 5-6: The DC of the vertical component computed corresponding to synthetic model 2 as a function of frequency. The spectra show multiple modes of excited Scholte waves which match with the theoretical one (red line).

On figure 5-7, the result of the LCI is shown. It is observed that the inverted model approaches the experimental Vs model.

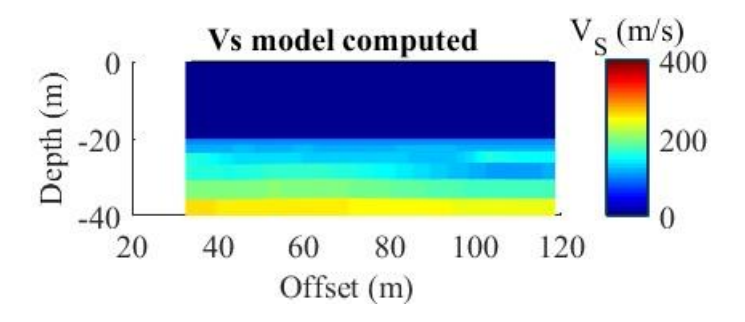


Figure 5-7: The estimated Vs model for the simple synthetic model using LCI

The comparison between the two is shown in Figure 5-8.

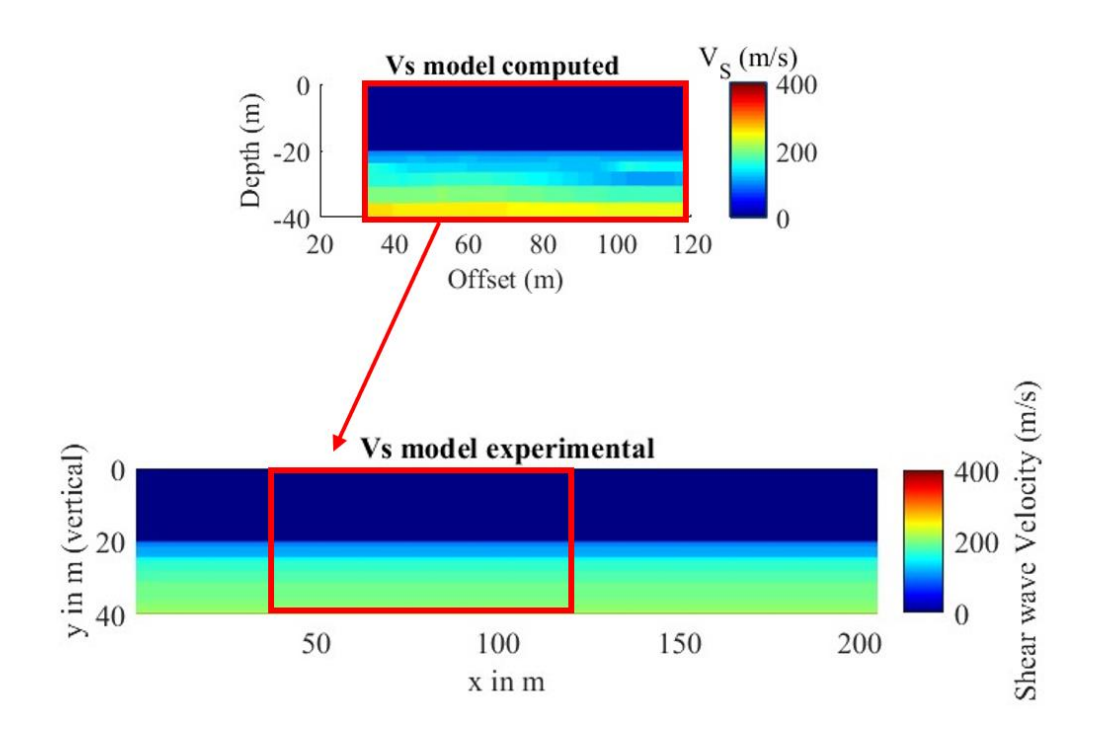


Figure 5-8: Comparison of experimental and computed Vs models for synthetic 2

5.3 Dataset number 3 DC and Inversion

The estimated phase-velocity spectra generated by the phase-shift method in the velocity-frequency (v-f) domain for the horizontal component are shown on Figure 5-9 and 5-10.

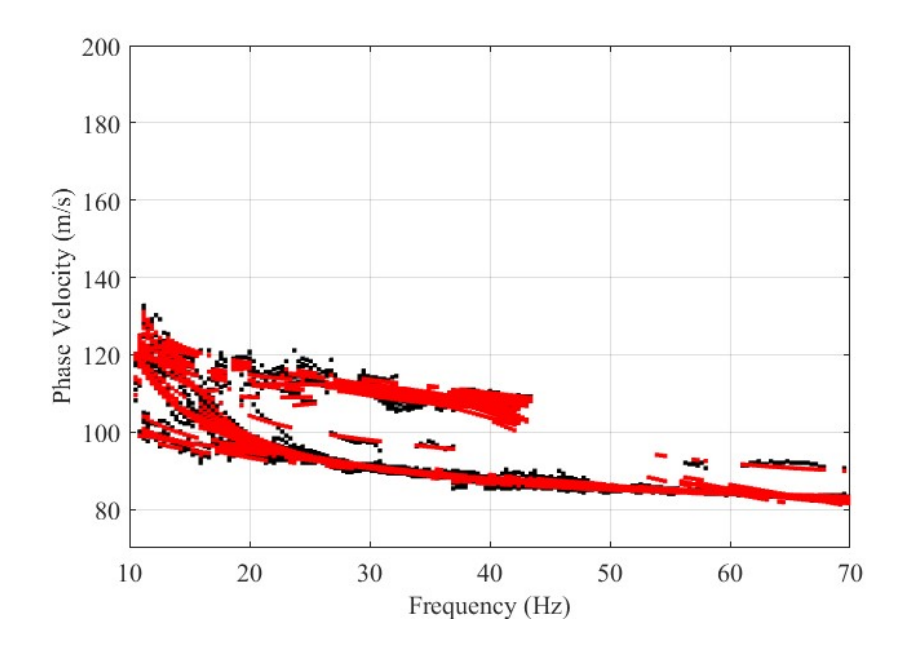


Figure 5-9: Computed DCs along with theoretical ones

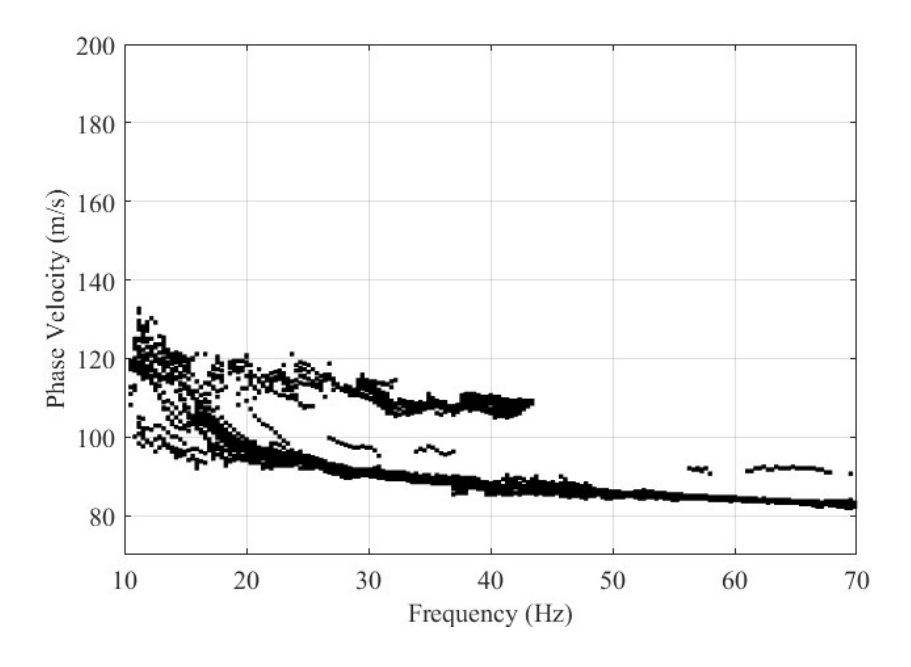


Figure 5-10: Cleaned DCs

On figure 5-11, the result of the LCI is shown. It is observed that the inverted model approaches the experimental Vs model.

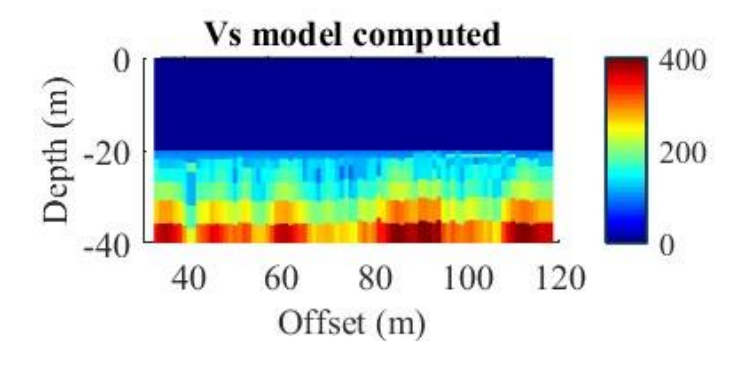


Figure 5-11: The estimated Vs model for the synthetic model 3 using LCI

The comparison between the two is shown in Figure 5-12. It can be observed that lateral variations can be spotted at the computed Vs model, with small precision.

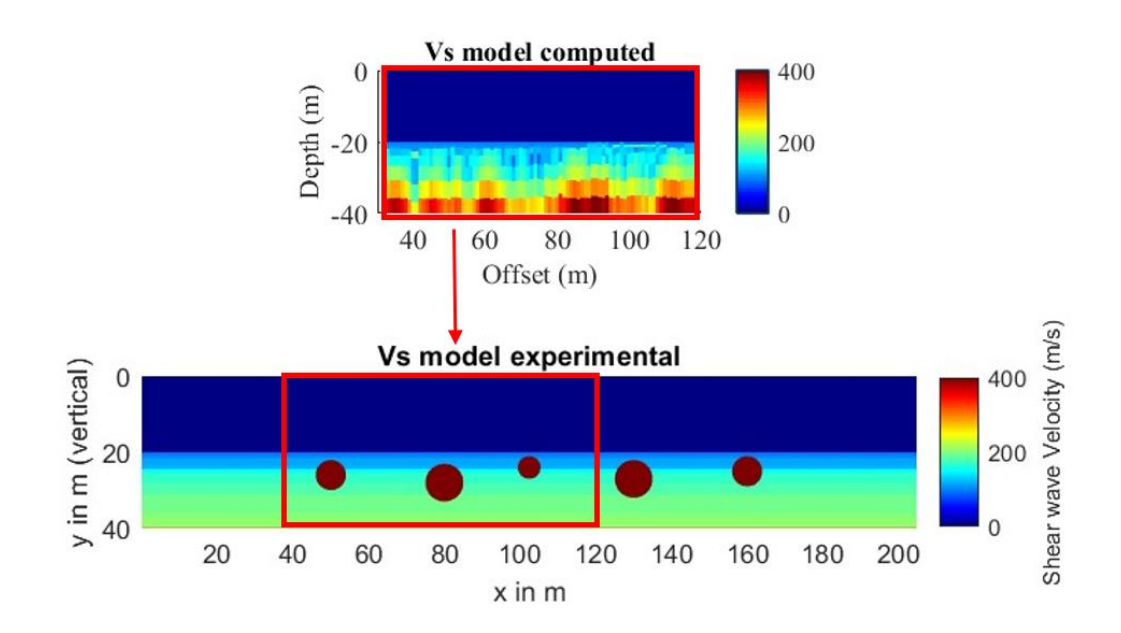


Figure 5-12: Comparison of experimental and computed Vs models for synthetic 3

6. Conclusions

6.1 Final Remarks

All in all, the aim of this thesis was met successfully. Three shallow marine models were simulated on SOFI3D software with experimental data: a simple 4 layered model, a model with real data from an anonymized area in South China Sea provided by Geowynd and the last one where lateral variations were introduced in the form of boulders. For all three models, surface wave analysis was implemented, where the phase-shift method was able to process the evenly spaced receivers' traces and extract the DC through an autopicking process. After the phase velocity spectra were extracted, an LCI was implemented, in order to compute the Vs of the subsurface model and conclude the study.

It is observed that the method is able to detect the lateral heterogeneities that we introduced. The precision is not high but the velocity anomalies are clearly shown on the computed model. The retrieved Vs values are compatible with the ground truth. Bigger lateral heterogeneities are easier to spot, while the smaller diameter boulders are not. Also, the resolution is higher for heterogeneities close to the seabed surface rather than the ones buried deeper.

During the creation of the simulated models the optimisation of the results was taken into account. We encountered many technical limitations which shaped the dimensions and parameters used for the models. In the end, the computed results match the ground truth and the Scholte waves dispersion can be used to detect seabed variations. It is a low-cost method that will optimise the study of a marine environment and can potentially give high resolution data to geotechnical studies for the construction of off shore wind turbine sites, a technology that will boost both sustainability and renewable energy.

6.2 Future Prospects

There are many ways with which this study can be enriched for future studies. To begin with, I would propose the use of a different numerical simulation software that depicts a marine environment more accurately, that will give more flexibility in the positioning of the receivers and source configuration as well as the size of the model. When it comes to processing of the data, a different inversion method of the DC can be used, like Monte Carlo, to increase the

resolution. Due to its high computational time, only LCI was used as the optimal inversion algorithm and indeed the quality of the results was good. Another idea to enrich this study is to increase the complexity of the model by placing boulders with both different petrophysical properties and scattered in different positions along the horizontal direction and also to use visco-elastic wave propagation equations instead of elastic, as used in this case for the sake of simplicity.

The Scholte waves can be studied in terms of environmental noise. A small step further from the purpose of this thesis would be to observe the Scholte wave energy dispersion while the wind turbine site is active and producing electricity.

7. References

- Aki, K, and P.G. Richards. 1980. Quantitative Seismology. Freeman and Co. Press New York.
- Auken, E., and A.V. Christiansen. 2004. *Layered and laterally constrained 2D inversion of resistivity data*. Geophysics, 69, 752-761.
- Bachrach, R, and A Nur. 1998. "High-resolution shallow-seismic experiments in sand, Part I: Water table, fluid flow, and saturation." (GEOPHYSICS, P. 1225–1233) 63 (4).
- Barrett, J, S. Pye, and S. et al Betts-Davies. 2022. "Energy demand reduction options for meeting national zero-emission targets in the United Kingdom." *Nat Energy* 7 726-735.
- Bohlen, Thomas, Denise De Nil, Daniel Kohn, and Stefan Jetschny. 2015. *SOFI3D seismic modeling with finite differences, 3D acoustic and viscoelastic version.* Karlsruhe Institute of Technology.
- Brossier, R., S. Operto, and J. Virieux. 2009. "Robust elastic frequency-domain full-waveform inversion using the L1 norm." (Geophys. Res. Lett., 36, L20310).
- Fang, Zhilong, Hongjian Fang, and Laurent Demanet. 2020. Chapter Five Deep generator priors for Bayesian seismic inversion. Vol. 61, in Advances in Geophysics, Pages 179-216.
- Haskell, N. 1953. "The dispersion of surface waves on multilayered media." *Bulletin of the Seimological Society of America*, 43, 17-34.
- Klein, Gerald, Thomas Bohlen, Friedrich Theilen, Simone Kugler, and Thomas Forbriger. 2005. "Acquisition and Inversion of Dispersive Seismic Waves in Shallow Marine Environments." *Mar Geophys Res* 26, 287–315.
- Kugler, S., and T. Bohlen. 2007. "Scholte-wave tomography for shallow-water marine sediments." (Geophysical Journal International, 168(2), 551–570).
- Kugler, Simone, Thomas Bohlen, Thomas Forbriger, Sascha Bussat, and Gerald Klein. 2007. "Scholte-wave tomography for shallow-water marine sediments." *Geophysical Journal International, Volume 168, Issue 2,* (Geophysical Journal International, Volume 168, Issue 2, February 2007, Pages 551–570) 551-570.

- Levander, A.R. 1988. "Fourth-order finite-difference P-SV seismograms." (Geophysics, 53(11), 1425–1436).
- Park, Choon B., R.D Miller, and Jianghai Xia. 1999. "Multichannel analysis of surface waves." (GEOPHYSICS, VOL. 64, NO.3, P. 800-808,).
- Potty, G.R., J.H. Miller, YT. Lin, and K. Vigness-Raposa. 2023. "Interface Wave Contribution to Acoustic Particle Motion During Offshore Wind Farm Construction." In *The Effects of Noise on Aquatic Life, pp 1-9*.
- Sambridge, M., and K. Mosegaard. 2002. *Monte Carlo Methods in Geophysical Inverse Problems*. Reviews of Geophysics, 40, 1-29.
- Socco, L.V., and C. Strobbia. 2004. "Surface-wave method for near-surface characterization: a tutorial."
- Socco, L.V., D. Boiero, S. Foti, and R. Wisen. 2009. *Laterally constrained inversion of ground roll from seismic reflection records*. Geophysics, 74, 35-45.
- Steeples, D.W., and Miller R.D. 1998. "Seismic Reflection Methods Applied to Engineering, Environmental and Groundwater Problems."
- Strobbia, L.C., A. Godio, and G. De Bacco. 2006. *Interfacial waves analysis for the geotechnical characterisation of marine sediments in shallow water.* Bollettino di Geofisica Teorica ed Applicata. 47. 145-162.
- Thomson, W.T. 1950. "Transmission of elastic waves through a stratified solid medium."
- Virieux, J. 1986. "P-SV wave propagation in heterogeneous media: velocity-stress finite difference method." (Geophysics, 51(4), 889–901).
- Wisen, Roger, and V Christiansen. 2005. "Laterally and Mutually Constrained Inversion of Surface Wave Seismic Data and Resistivity Data ." *Journal of Environmental and Engineering Geophysics 2005 10:3, 251-262*.
- Zheng, Yingcai, Xinding Fang, Jing Liu, and Michael C. Fehler. 2013. *Scholte waves* generated by seafloor topography. Massachusetts Institute of Technology: Department of Earth, Atmospheric, and Planetary Sciences.